geosciences

MDPI

Article

Morphosedimentary, Structural and Benthic Characterization of Carbonate Mound Fields on the Upper Continental Slope of the Northern Alboran Sea (Western Mediterranean)

Olga Sánchez-Guillamón [1,*], Jose L. Rueda [1], Claudia Wienberg [2], Gemma Ercilla [3], Juan Tomás Vázquez [1], Maria Gómez-Ballesteros [4], Javier Urra [1], Elena Moya-Urbano [5], Ferran Estrada [3] and Dierk Hebbeln [2]

1 Centro Oceanográfico de Málaga, Instituto Español de Oceanografía (IEO-CSIC), 29640 Fuengirola, Spain; jose.rueda@ieo.es (J.L.R.); juantomas.vazquez@ieo.es (J.T.V.); javier.urra@ieo.es (J.U.)
2 MARUM—Center for Marine Environmental Sciences, University of Bremen, LeobenerStraße 8, 28359 Bremen, Germany; cwberg@marum.de (C.W.); dhebbeln@marum.de (D.H.)
3 Continental Margins Group, Institut de Ciencies del Mar-CSIC, Passeig Marítim de la Barceloneta 37-49, 08003 Barcelona, Spain; gemma@icm.csic.es (G.E.); festrada@icm.csic.es (F.E.)
4 Servicios Centrales de Madrid, Instituto Español de Oceanografía (IEO-CSIC), 28002 Madrid, Spain; maria.gomez@ieo.es
5 Departamento de Biología Animal, Universidad de Málaga, 29071 Málaga, Spain; emoyaurbano@gmail.com
* Correspondence: olga.sanchez@ieo.es

check for updates

Citation: Sánchez-Guillamón, O.; Rueda, J.L.; Wienberg, C.; Ercilla, G.; Vázquez, J.T.; Gómez-Ballesteros, M.; Urra, J.; Moya-Urbano, E.; Estrada, F.; Hebbeln, D. Morphosedimentary, Structural and Benthic Characterization of Carbonate Mound Fields on the Upper Continental Slope of the Northern Alboran Sea (Western Mediterranean). *Geosciences* **2022**, *12*, 111. https://doi.org/10.3390/geosciences12030111

Academic Editors: Peter Feldens and Jesus Martinez-Frias

Received: 6 February 2022
Accepted: 24 February 2022
Published: 28 February 2022

Abstract: Carbonate mounds clustering in three fields were characterized on the upper continental slope of the northern Alboran Sea by means of a detailed analysis of the morphosedimentary and structural features using high-resolution bathymetry and parametric profiles. The contemporary and past benthic and demersal species were studied using ROV underwater imagery and some samples. A total of 325 mounds, with heights between 1 and 18 m, and 204 buried mounds were detected between 155 to 401 m water depth. Transparent facies characterize the mounds, which root on at least six erosive surfaces, indicating different growth stages. At present, these mounds are covered with soft sediments and typical bathyal sedimentary habitat-forming species, such as sea-pens, cerianthids and sabellid polychaetes. Nevertheless, remains of colonial scleractinians, rhodoliths and bivalves were detected and their role as potential mound-forming species is discussed. We hypothesized that the formation of these mounds could be related to favorable climatic conditions for cold-water corals, possibly during the late Pleistocene. The occurrence on top of some mounds of abundant rhodoliths suggests that some mounds were in the photic zone during minimum sea level and boreal guest fauna (e.g., *Modiolus modiolus*), which declined in the western Mediterranean after the Termination 1a of the Last Glacial (Late Pleistocene).

Keywords: carbonate mounds; geomorphology; benthos; habitats; rhodoliths; *Modiolus modiolus*; Alboran Sea

1. Introduction

Carbonate mounds are sedimentary seafloor elevations that have been detected worldwide, rise up to a few meters and up to 380 m [1] (above the surrounding seabed) and displaying different shapes (e.g., round, elongated), sizes (spanning from 10 s to 1000 s m in diameter) and sedimentary composition [2–6]. They often cluster as extended fields along continental shelves and slopes (from 100 to 1000 m water depth) comprising tens and even <1000 mounds [7,8]. Carbonate mounds are formed by framework-building calcareous organisms distributed according to various transport, depositional and erosive processes [2,4,5]. Hence, they are firstly dependent on the biological activity of their reef-forming organisms, which include colonial suspension feeding invertebrates, such as cnidarians (e.g., scleractinians, stony hydrozoans and octocorals) [9,10], sponges [11], serpulids [12] and bryozoans [13]. These framework-building organisms sometimes have

branching forms, increasing the complexity and diversity of substrates, food sources and associated sessile and mobile organisms, including those with calcareous skeletons (e.g., encrusting coralline algae, mollusks, cirripeds, etc.) [14–17]). Indeed, these associated organisms with calcareous skeletons may also contribute to the accretion of the carbonate mound. Thus, the heterogeneous composition of carbonate mounds includes fragments of the habitat-forming species as well as other parautochthonous bioclasts, embedded in hemipelagic and contouritic sediments [15–18].

One of the most common and dominant faunal groups forming carbonate mounds are colonial cold-water corals (CWCs), which are dependent on different physicochemical parameters, such as temperature, salinity, dissolved oxygen concentrations, aragonite saturation and water mass density [10,19–25]. Nevertheless, CWC growth is also linked to the food availability (phytoplankton, zooplankton, particulate organic material), promoted by enhanced surface productivity and by the local hydrodynamic regime (including geostrophic currents, internal tides and waves, cascading and down-welling processes) supporting the lateral advection of food particles to the sessile CWC [26–31]). In general, CWCs develop reefs in areas with vigorous bottom currents (sometimes >50 cm s^{-1}), preventing them from smothering by sediments [10,27,28,32,33]. The three-dimensional structure of CWCs can baffle suspended sediments entering their framework over time, and the continuous interplay between this sediment baffling and CWC growth leads to the formation of CWC mounds [18,20,33,34]. In general, CWC mounds maintain sustained development through time if there is equilibrium between sediment and food supply; often CWC mounds display an internal structure related to recurring periods of CWC colonization, decline and renewed colonization related to environmental changes induced by the Late Quaternary climatic cycles [18,35–39]. Periods of growth and/or decline of CWCs have been linked to changes in the physicochemical properties and productivity of the water masses [35,38,40–46]. Bottom currents can also create small erosional and depositional sedimentary structures and modulate the shape of the mound [47]), resulting in flattened top mounds (within the storm wave base), cone-shaped mounds (quiet and deeper waters) [4], elongated mound shapes (due to the preferred growth of the reef-forming organisms towards the main current) [48]), and mounds with current scours and moats around them (in strong bottom deep water along slope bottom currents) [35,41,49–51]. Active CWC mounds are covered by thriving CWC reefs and background sedimentation rate is generally lower than CWCs growth rate, however, contouritic and/or hemipelagic sediments have generally been found as major structural components contributing to the accretion of the CWC mounds (sometimes representing up to two-thirds of the mound deposits) [18,52,53]. Favorable environmental conditions for CWC growth or increases of background sedimentation in specific areas or time periods (e.g., sediment outputs from meltwater during deglaciation, changes in bottom current regimes, sediment extrusion in mud volcanoes, etc.) may promote the collapse and burial of the CWC reefs and their associated biota, resulting in the stagnation of the CWC mounds [7,38,43,54,55].

The analysis of high-resolution geomorphological and sedimentary data obtained by geophysical techniques since the 2000s has improved the knowledge about Quaternary sedimentation in the Alboran Sea. Some of these studies highlighted the role of contourite erosional and depositional processes in the formation of contourite terraces and drifts along the Spanish and Moroccan continental slopes [6,56]. These contouritic terraces that shape the continental slope are formed by turbulent processes (i.e., internal waves) occurring at the interfaces between the Atlantic and Mediterranean waters through the Quaternary glacio-eustatic sea-level changes [56,57]. In addition, other studies revealed a large scale distribution of clustered mounds with circular to elongated footprints along the Alboran Sea margins [43,55,58–61]. The clustering of mounds in extensive fields, especially along the upper and middle slopes, has been recently documented in the southern and central Alboran Sea, especially in the East [43,61] and West Melilla CWC mound provinces [46,55], as well as in the Cabliers bank [62,63] (Figure 1A). Furthermore, three mound fields have been located within the contouritic terraces of the northern Alboran Sea margin (south-

eastern Spain), in front of Marbella (around the Torrenueva submarine canyon), in front of Málaga and southwest off Almería [6,58,59,64]. Sampling and direct observations of the southern Alboran Sea carbonate mounds (East and West Melilla CWC mound provinces) confirmed that CWCs were the main organism involved in their formation [15,43,46,55]. Nevertheless, some of those CWC mounds are nowadays partly or even completely buried by contouritic and hemipelagic sediments [55,56,65]. The distribution and burial state of the observed CWC mounds were explained by changes in water mass dynamics during the Late Quaternary climatic cycles [15,43,46].

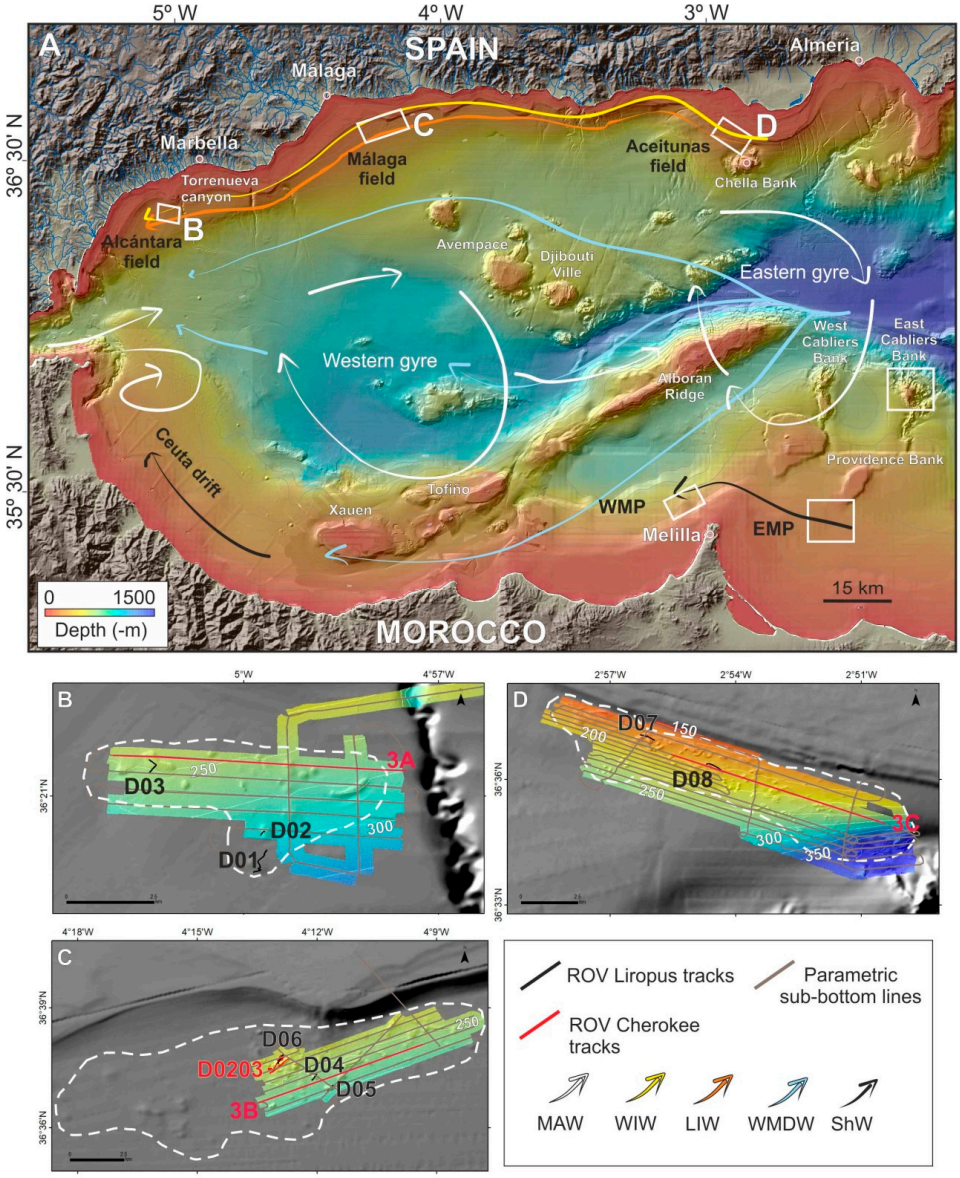

Figure 1. (**A**) Overview map showing the three carbonate mound fields (**B**–**D**) on the northern margin of the Alboran Sea described in this study and the location of cold-water corals (CWC) mound provinces detected in the southern Alboran Sea (Cabliers, West Melilla (WMP) and East Melilla (EMP) mound provinces [55,61–63]. The water mass circulation scheme is adapted from [56] based on Legend: MAW, Atlantic Water; WIW, Western Intermediate Water; LIW, Levantine Intermediate Water; WMDW, Western Mediterranean Deep Water; ShW, Shelf Water. Bathymetric map of (**B**) Alcántara carbonate mound field; (**C**) Málaga carbonate mound field and (**D**) Aceitunas carbonate mound field showing the location of dive tracks and sub-bottom parametric profiles (lines). Extension of the mound fields are marked by white dotted contours. The black scales represent 2.5 km. Bathymetric contours with 25 m spacing are shown as white lines.

The northern Alboran Sea mounds were initially identified on high-resolution bathymetric maps during the analysis of the main morphotectonic characteristics of this margin [58,59]. Subsequently, some of the mounds located in front of Málaga were investigated using a Remotely Operated Vehicle (ROV) during a German expedition with the R/V POSEIDON (POS385, led by MARUM) [60]. Later on, two multidisciplinary projects (MONCARAL and RIGEL) from the Instituto Español de Oceanografía (IEO) provided a new opportunity for exploring the different mounds of the northern Alboran Sea margin during two expeditions with the R/V ÁngelesAlvariño (MONCARAL 0516 and RIGEL 1116). Both geological and biological sampling was carried out, together with the acquisition of high-resolution acoustic datasets (bathymetry and parametric seismic profiles) and of underwater images using a ROV.

The main aim of the present study is to provide a detailed analysis of the morphosedimentary features, internal structure and contemporary and past benthic and subordinate organisms, including some habitat-forming species, of the three different mound fields located in the contouritic terrace, developed along the upper continental slope of the northern Alboran Sea [56–58]. The new datasets improve the knowledge of the morphology, distribution and the present-day and past evolution of these mounds in relation to some geological and oceanographic processes.

2. Regional Setting

The tectonic evolution of the Alboran Sea Basin (western Mediterranean Sea), linked to the Betics-Rif orogeny, has generated a basin characterized by narrow continental shelves and irregular, steep to gentle slopes, and a series of ridges and seamounts, of volcanic and/or tectonic origin, such as Xauen, Djibouti Ville and Avempace, which increase the seafloor complexity of the basin (Figure 1A) [6,66]. As mentioned previously, the upper continental slope is characterized by a contouritic terrace [56].

In the Alboran Sea, intermediate and deep Mediterranean waters migrate to the west through the Strait of Gibraltar, through which surficial Modified Atlantic Water (MAW) enters and flows to the east [67]. The MAW forms two anticyclonic gyres in the Alboran Sea (Western and Eastern Alboran Gyres) that extend to maximum depths of 150 to 200 m [68]. The Mediterranean water masses have been grouped by density [69] into two large groups [56]: (i) Light Mediterranean Water (LMW) comprising the less dense and salty intermediate waters that include the Western Intermediate Water (WIW), which flows at depths between 150 and 200 mbsl, the Levantine Intermediate Water (LIW), between 200 and 500 m water depth, and the lighter top of the Tyrrhenian Deep Water which flows below 500 m; and (ii) Dense Mediterranean Waters (DMW) including the lower part of the Tyrrhenian Deep Water and the Western Mediterranean Deep Water that flow below 600 m water depth. Both, the LMW and the DMW interact with the bottom of the basin: the LMW flows preferentially along the northern Alboran margin generating an erosive terrace at its interface with the MAW (around 150–300 m water depth) and a series of attached drifts along the slope or around the seamount-like banks and ridges; while the DMW circulates throughout the basin but ascends to shallower depths along the southern Alboran Sea margin, controlling the formation of the Ceuta Drift [56].

The Alboran Sea is one of the most productive areas within the generally oligotrophic Mediterranean Sea and its productivity is partially driven by local nutrient-rich upwellings that occur along the edge of the Western Alboran Gyre and at the eastern limb of the Eastern Alboran Gyre [68,70,71]. Some rivers discharge into the Alboran Sea, with the large Moulouya river at the Moroccan margin and the Guadiaro, Guadalhorce, Guadalfeo and Andarax rivers at the Spanish margin being the most important ones.

Due to the oceanographic and geological complexity of the Alboran Sea, a large variety of habitats and associated species from different biogeographical regions occur in the basin, representing a biodiversity hotspot for the European and northern African margins [72]. One of the most biodiverse habitats in bathyal depths of the basin is represented by reefs dominated by CWCs, which have been detected on various seafloor structures including

seamounts (e.g., Seco de los Olivos (Chella Bank), East and West Cabliers, Djibouti Ville), mud volcanoes, submarine canyons and carbonate mounds [15,43,54,60,62,73,74]). Only rare occurrences of CWCs are reported for the Alboran Sea during the Last Glacial, but during the last deglaciation since the onset of the Bølling-Allerød warm interval, CWCs experienced a marked proliferation, which resulted in enhanced mound aggradation as indicated for several CWC mounds in the southern Alboran Sea [15,43,46]. The deglacial proliferation of CWCs coincided with enhanced surface ocean productivity and a peak in meltwater discharge originating from the northern Mediterranean borderlands, which caused a major re-organization of the Mediterranean thermohaline circulation [43,75]. Enhanced mound formation in the southern Alboran Sea lasted until the Early Holocene [15,43,46], which was likely controlled by strong hydrodynamic conditions caused by internal waves that developed along the density gradient between the Atlantic and Mediterranean waters [43,46]. Internal waves generally promote the resuspension and transport of recently deposited and/or fresh food particles at an increased velocity to the CWCs thriving on the mounds and, thus, enhance the chance of the CWC polyps to capture these particles [18,27]. Since the late Early to Mid-Holocene mound formation significantly slowed-down due to relatively weak hydrodynamics and oligotrophic conditions, and eventually stagnated until today with some of them becoming (partially to completely) buried by sediments [46].

3. Materials and Methods

In May 2009, during the expedition POS-385 on board the German R/V Poseidon [60]; two video transects (Dives 02 and 03 in Figure 1C) were performed crossing some of the mounds off Málaga with the MARUM ROV Cherokee. The ROV was equipped with four video cameras including a color video zoom camera and a digital still camera. The cameras were further equipped with three laser pointers for scaling adjusted to 19.5 cm in the horizontal direction and 12 cm in the vertical direction, and a hydraulically operated manipulator for collecting fauna and rock samples. A total of 3.5 h of video footage were recorded along more than 3000 m of seafloor tracks (Table 1). The ROV transects were carried out at low speed and close to the seafloor.

Table 1. Metadata of the ROV video transects recorded during POS-385 (ROV Cherokke) and MONCARAL 0516 (ROV Liropus 2000) expeditions in the northern Alboran Sea.

Expedition	Mound Field	Dive	Track Length (m)	Water Depth (m)	Start Coordinates	End Coordinates
POS-385	Málaga	02	1128	243–233	36°37.35′ N 04°13.16′ W	36°37.72′ N 04°12.69′ W
POS-385	Málaga	03	1931	236–218	36°37.48′ N 04°13.10′ W	36°37.78′ N 04°12.91′ W
MONCARAL	Alcántara	01	2512	309–317	36°19.83′ N 04°59.85′ W	36°20.17′ N 04°59.65′ W
MONCARAL	Alcántara	02	353	291–297	36°20.40′ N 04°59.74′ W	36°20.46′ N 04°59.69′ W
MONCARAL	Alcántara	03	1452	243–253	36°21.35′ N 05°01.46′ W	36°21.56′ N 05°01.46′ W
MONCARAL	Málaga	04	1307	238–261	36°37.20′ N 04°12.13′ W	36°37.34′ N 04°12.01′ W
MONCARAL	Málaga	05	1895	271–276	36°36.90′ N 04°11.73′W	36°37.06′ N 04°11.60′ W
MONCARAL	Málaga	06	1586	225–230	36°37.61′ N 04°12.97′ W	36°37.83′ N 04°12.84′ W
MONCARAL	Aceitunas	07	1348	180	36°36.94′ N 02°55.95′ W	36°37.06′ N 02°56.27′ W
MONCARAL	Aceitunas	08	1192	194–200	36°36.18′ N 02°54.28′ W	36°36.37′ N 02°54.71′ W

In May 2016, the expedition MONCARAL 0516 on board R/V Ángeles Alvariño (IEO, Spain) explored three mound fields of the northern continental slope of the Alboran Sea. These three fields have been named in the present study, from west to east, as Alcántara, Málaga and Aceitunas mound fields. Bathymetric data were obtained with a Kongsberg EM710 multibeam echosounder system, covering a total area of 102 km^2 between 142 and 408 m water depth (Figure 1B–D). At the same time, high-resolution parametric

profiles were acquired using a TOPAS PS018. Multibeam data were imported in a single project using CARIS HIPS and SIPS V. 11.1 software (© Teledyne) and were georeferenced to create a gridded base surface of 5 m cell size. After that, it was integrated into an ArcGIS v.10.8 (© ESRI) project where the geomorphological analyses were made. These geomorphological analyses include morphometric characterization after computing main size, slope and shape parameters, such as height, axis length and irregularity of the mounds (Iri), which represents the contour complexity of the polygon of each mound [76] (Table 2), as well as mound counting and Kernel density of the fields (mounds per km^2). Parametric profiles were loaded in Kingdom IHS Markit software for the interpretation of seafloor and subseafloor structures.

Table 2. Location, number (N°) and morphological features of the mounds and mound fields detected in the northern Alboran Sea (Iri: Irregularity index, BA: Basal Area, H: Height).

Mound Field	Location	Depth Range (m)	N° of Exposed Mounds	N° of Buried Mounds	Length Range (m)	Width Range (m)	Iri Range	BA (km^2)	H Range (m)	Mean Slope (°)
Alcántara	North-western Alboran Sea	239–297	18	26	131–966	84–361	1.3–3.1	0.82	3–14	2.5–6
Málaga	North-central Alboran Sea	220–273	64	58	79–831	57–313	1.03–4.7	1.33	2–18	2.5–16
Aceitunas	North-eastern Alboran Sea	155–401	243	120	6–630	5–295	1.03–3.5	3.08	1–15	2–20
All mound fields		155–401	325	204	6–966	5–361	1.03–4.7	5.23	1–18	2–20

Eight video transects (Dives 01 to 08) were recorded using the ROV Liropus 2000 at the three carbonate mound fields (Figure 1B–D) providing a total of 10 h of high-resolution underwater imagery along almost 12,000 m of seafloor tracks (Table 1). The ROV transects were carried out at low speed and close to the seafloor. This ROV was equipped with a full HD camera, two laser pointers for scaling (10 cm between them) and two hydraulic manipulators for collecting samples of rocks, sediment, fauna and remains of organisms. Samples collected during the ROV dives were used for identifying seafloor features and organisms observed in the underwater images. Qualitative analysis of video transects was carried out using VLC Media Player 3.0.16 for Windows software. The video fragments were viewed for identification of benthic and demersal species, substrate type categories (i.e., mud, sand, gravel, bioclasts and consolidated rocks) and sedimentary bedforms (i.e., moats). Furthermore, eleven surface sediment samples (VV01-VV11) were recovered from the three mound fields and adjacent bottoms between 173 and 317 m depth using a Van Veen grab sampler (Appendix A).

Finally, in November 2016, the expedition RIGEL 1116 on board R/V Ángeles Alvariño sampled the top and flanks of some of the mounds detected during the previous expeditions. Nine surface sediment samples (VV16-VV24) using a Van Veen grab sampler and nine sediment cores (TG16-TG24) using a gravity corer were obtained from the Málaga and Aceitunas mound fields between 188 and 255 m and 171 and 248 m depth. The maximum recovery of the gravity cores was 38 cm at the mounds and 260 cm at the adjacent seafloor. These samples were only used for in situ characterization of the top subseafloor sediments/structures (Appendix A).

4. Results

4.1. Alcántara Mound Field

The Alcántara mound field in the west is located at the western side of the Torrenueva canyon system, 11 km off the coast, between 239 to 297 m water depth (Figure 1B). It is the smallest mound field of the northern Alboran Sea and it is composed of 18 mainly elongated mounds stretching NW-SE, NE-SW and N-S with a mean Irregularity index (Iri) of 1.7. The mounds have heights of up to 14 m, with maximum slopes up to 18° and diameters between 131 to 966 m (Figure 2). This field contains the most elongated mounds of the northern Alboran Sea, and often these elongated mounds display higher reliefs (up

to 14 m) than the circular ones that are generally lower and smoother (Table 2). In plain view, this field shows a random spatial distribution of individual mounds. In general, the mounds are highly separated with a low mound density (ca. 1 mound per km^2) although the central sector of the field contains a cluster of mounds with a higher density (up to 8) (Figure 2D). Furthermore, the most elongated mounds seem to be composed of merged smaller mounds and occasionally, those elongated mounds are surrounded by moats down to 3 m in relation to the surrounding seabed (e.g., at the eastern sector of the Alcántara mound field) (Figures 2A and 3).

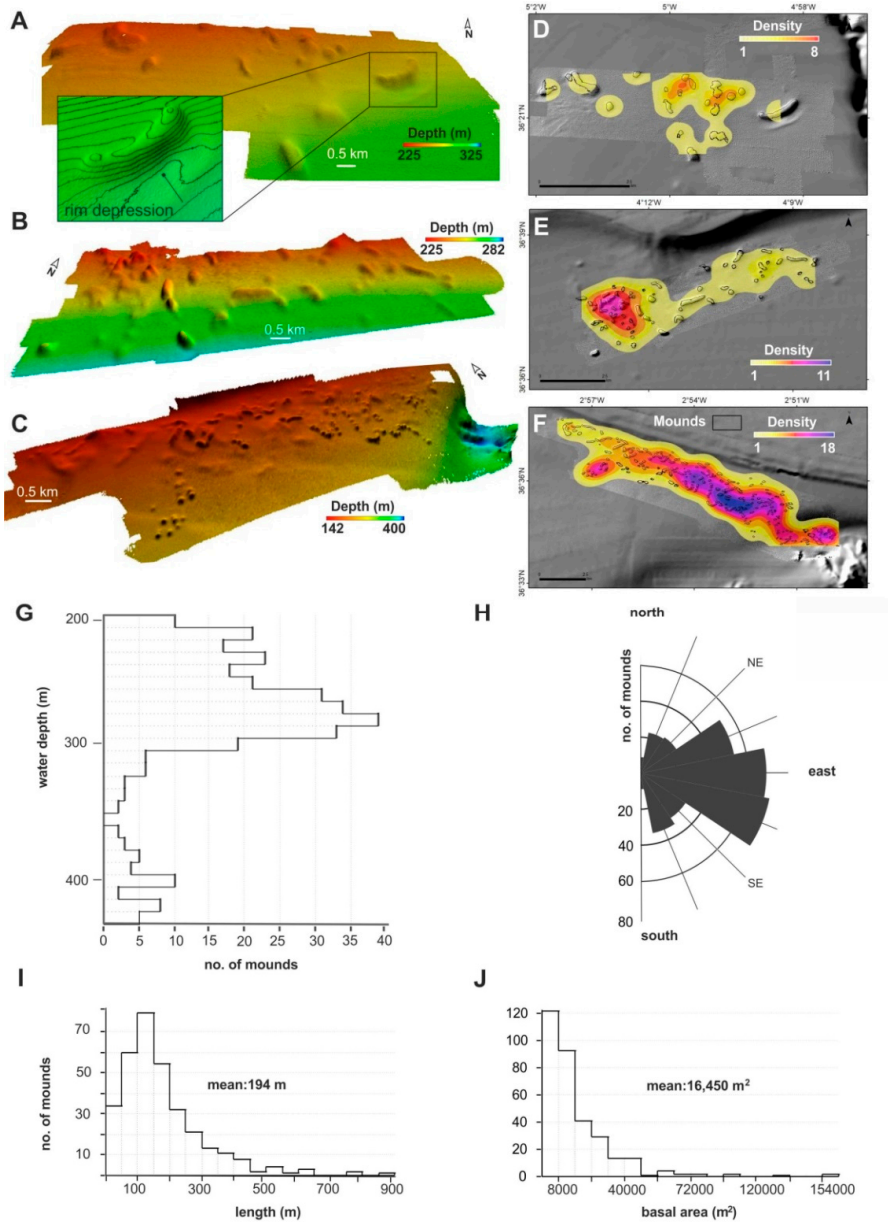

Figure 2. Spatial distribution and main morphological variables of the 325 carbonate mounds detected in the three mound fields of the northern Alboran Sea. (**A**–**C**) 3D bathymetric images of the carbonate mound fields with a vertical exaggeration of 6. (**A**) Alcántara mound field; (**B**) Málaga mound field and (**C**) Aceitunas mound field. (**D**–**F**) Kernel density maps (mound per km^2) of the mound fields based on mound contours. The black scales represent 2.5 km. (**G**–**J**) Morphometric data of the analyzed geomorphological features: (**G**) Bathymetric distribution of carbonate mounds in terms of the number of mounds; (**H**) Main trends of length axes orientation of the carbonate mounds. Histograms show (**I**) the length and (**J**) the basal area covered by the mounds.

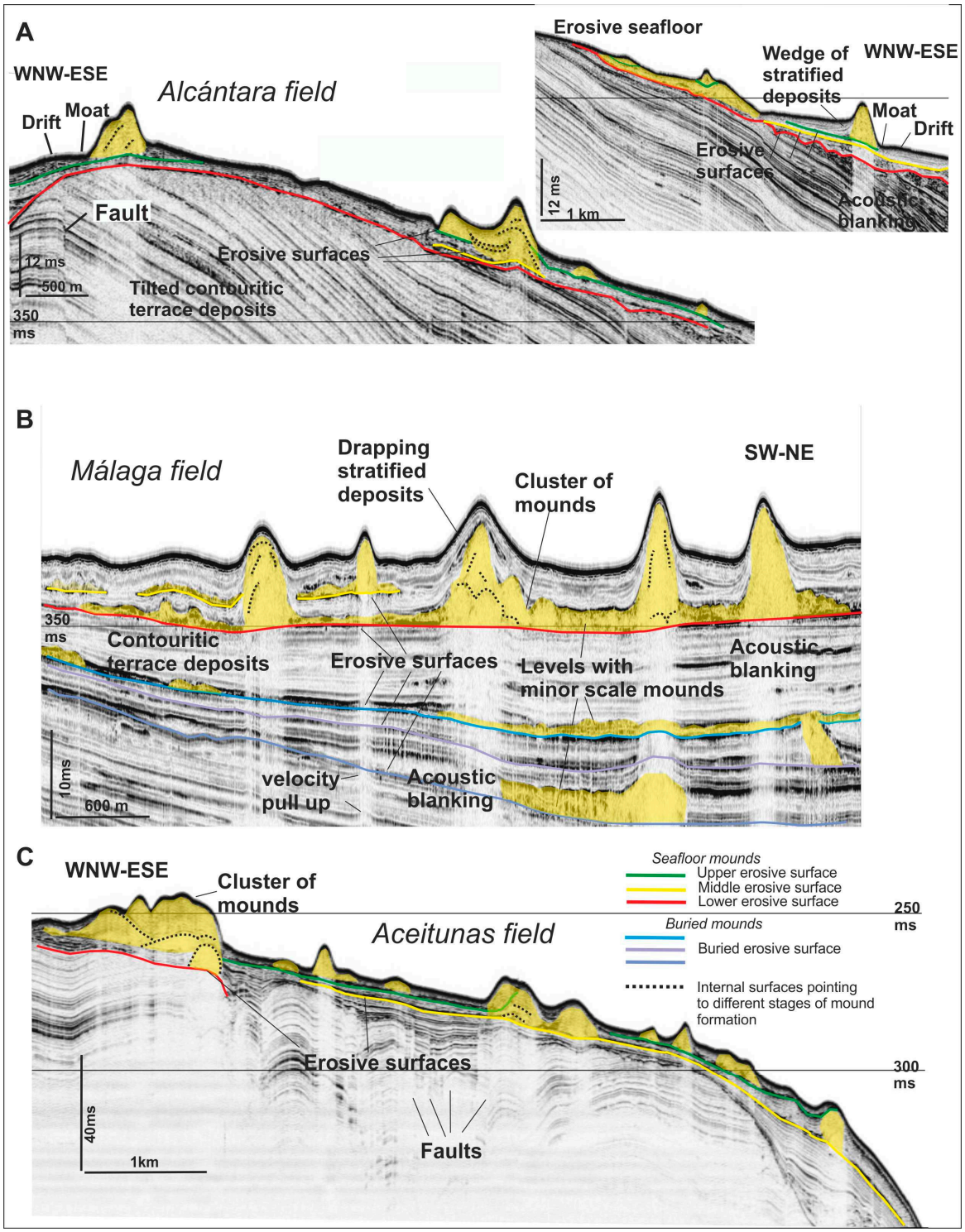

Figure 3. High-resolution sub-bottom parametric profiles showing some carbonate mounds and contourite drift sequences of the (**A**) Alcántara mound field; (**B**) Málaga mound field and (**C**) Aceitunas mound field in the northern Alboran Sea. Location of the profiles is shown in Figure 1B–D.

The three surface sediment samples VV01-04 recovered with the Van Veen grab from some of the Alcántara mounds are overall characterized by mud and muddy sands with high bioclastic content corresponding to the shells of dominant mollusks of bathyal muddy bottoms, such as *Nucula sulcata*, *Nassarius ovoideus*, *Abra* spp., among others (Appendix A). The main bottom sediments and benthic communities detected in Alcántara mound field

were bathyal muds and muddy sands with burrowing megafauna, mainly displaying a low-moderate number of burrows (1–5 burrows m^{-2}) of large decapods, such as *Munida* spp. and the Norway lobster (*Nephrops norvegicus*) (Dive 1; Figures 4 and 5). Small reducts of bathyal muds with seapens (mostly *Veretillum cynomorium*), cerianthiids (*Cerianthus* spp., *Arachnanthus* sp.) and sabellids (*Sabella pavonina*) have also been detected in specific areas of the mound field (Dive 3). Other benthic organisms detected at such sediment-covered bottoms were the hydrozoan *Nemertesia ramosa*, the sedentary polychate *Spiochaetopterus* sp., hermit crabs (*Dardanus* sp. and *Pagurus* sp.) and some pandalid shrimps (*Plesionika* spp.) as well as the gastropods *Fusiturris similis* and *Aporrhais serresiana*. Common fishes in this field are unidentified species of Myctophids, the horse mackerel *Trachurus* spp., the dogfish *Scyliorhinus canicula*, the Mediterranean silver scabbardfish *Lepidopus caudatus* and the boar fish *Capros aper*. Remains of solitary scleractinians (mainly *Caryophyllia* spp.) were also detected in the sediment. The main indicators of human anthropic activities were bottom-trawling marks on the seafloor of different sectors of the Alcántara mound field.

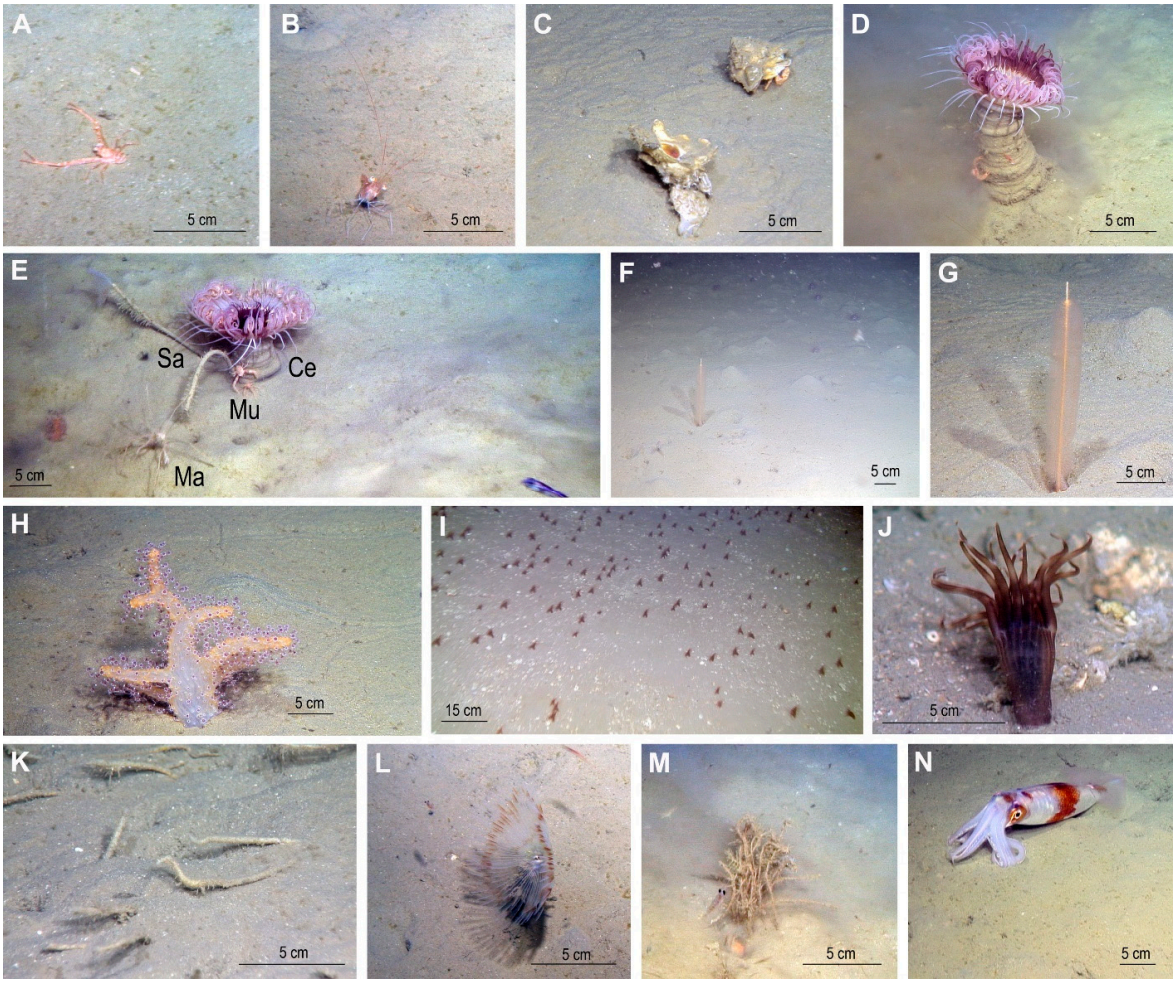

Figure 4. Some examples of present-day bottom sediments and benthic and demersal fauna detected at the Alcántara (**M**), Málaga (**A**–**E**,**L**,**N**) and Aceitunas (**F**–**K**) carbonate mound fields of the northern Alboran Sea. (**A**) the burrowing decapod *Munida* sp.; (**B**) the pandalid shrimp *Plesionika heterocarpus*; (**C**) Hermit crabs using *Xenophora crispa* shells; (**D**,**E**) *Cerianthus* sp. (Ce) individuals, with one of them located close to two sabellidpolychaete tubes (Sa) and the decapods *Munida* sp. (Mu) and *Macropodia* sp. (Ma); (**F**,**G**) the seapen *Virgularia mirabilis*; (**H**) the soft bottom octocoral *Alcyonum palmatum*; (**I**,**J**) an aggregation of an unidentified solitary anthozoan, including a close-up of one individual; (**K**,**M**) tubes of the polychaete *Spiochaetopterus* sp. colonized by small hydrozoans; (**L**) the sabellid polychaete *Sabella pavonina*; (**N**) the squid *Illex coindetii*. All underwater images obtained with ROV LIROPUS 2000, Instituto Español de Oceanografía (Spain).

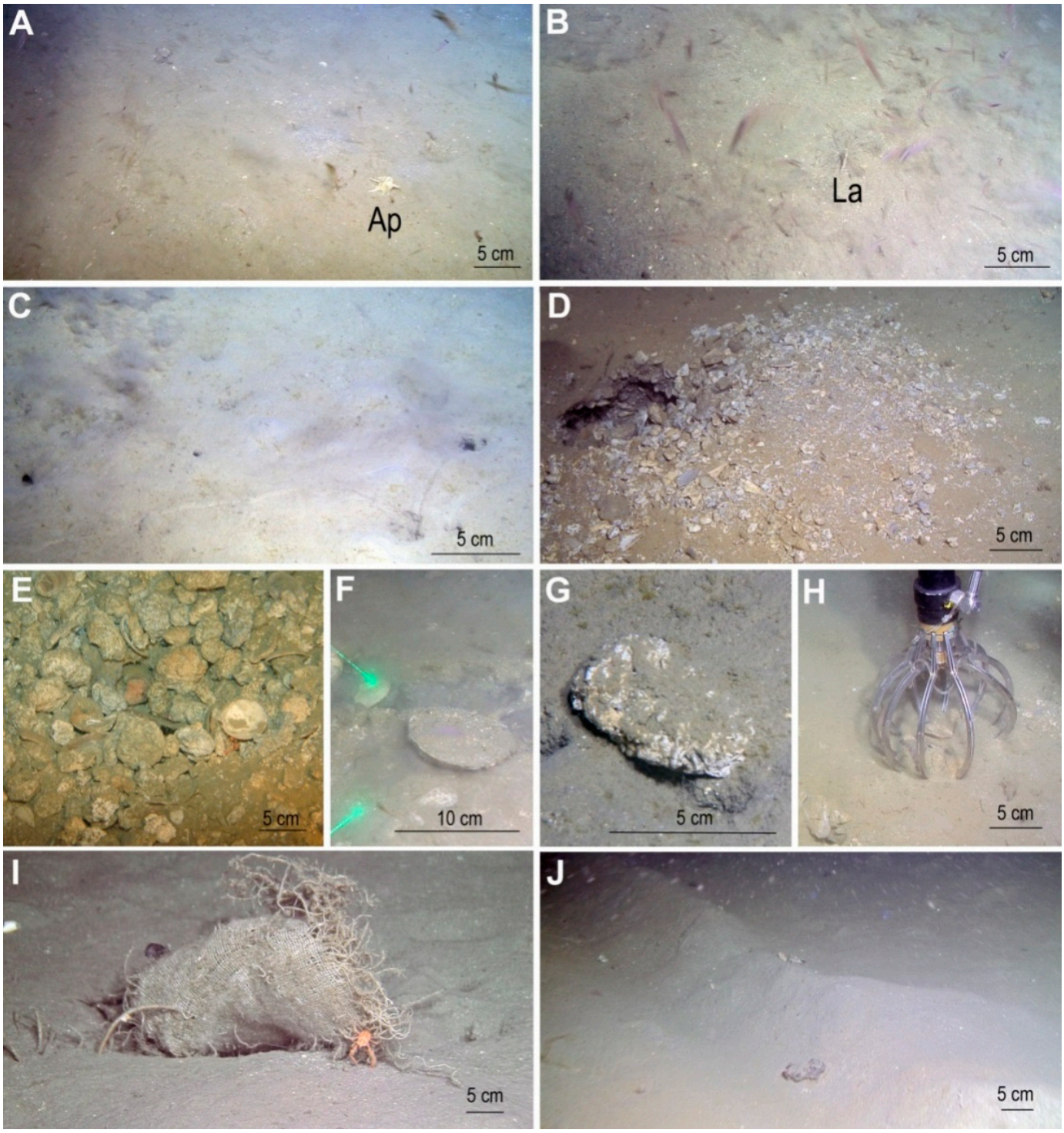

Figure 5. Some examples of present-day bottom sediments, fossil remains and anthropic activity indicators detected for the Alcántara (**A**,**B**), Málaga (**C**–**H**) and Aceitunas (**I**,**J**) carbonate mound fields of the northern Alboran Sea. (**A**,**B**) Muddy bottoms with some typical bathyal species, such as the gastropod *Aporrhais serresiana* (Ap) and the polychaete *Lanice conchilega* (La); (**C**) Bathyal muddy bottoms with burrowing megafauna (mainly *Munida* spp. and *Nephrops norvegicus*); (**D**–**H**) rhodoliths and bivalve remains detected in several mounds; (**I**) a cloth sack over *Spiochaetopterus* sp. tubes and (**J**) a bottom-trawling mark. All underwater images obtained with ROV LIROPUS 2000, Instituto Español de Oceanografía (Spain), except figure E obtained with ROV CHEROKEE, Marum, Bremen (Germany).

4.2. Malága Mound Field

The central Málaga mound field is located 35 km southeast off Málaga, between 220 and 273 m water depth (Figure 1C). This field consists of 64 mounds with mainly circular to elongated shapes, with the elongated mounds mainly displaying NW to SE extensions and a mean Iri of 2.1. The mounds have heights of 2 to 18 m, and diameters between 79 and 831 m with maximum slopes of 14°. The most elongated mounds generally display the largest heights (up to 18 m) as well as the steepest flanks and a mean Iri of 1.8 (Table 2). This field contains the largest number of mounds with the largest basal area (Table 2).

The spatial distribution of the mounds shows two different trends: mounds clustered in the western sector of the field with mound density values of 11 per km^2, and scattered mounds with much lower mound densities (less than 2) in the eastern sector (Figure 2E). In addition, even further to the west, another cluster of mounds could be identified on the hillshade map (Figure 1C) but the scarce data resolution did not allow its detailed and comparative analysis.

The sediment surface samples VV05-08 and VV22-24 taken from the Málaga mound field consisted of mud and muddy sand with some bioclasts, mainly rhodoliths and fragmented bivalves and polychaete tubes, such as *Aporrhais serresianus, Nassarius ovoideus, Neopycnodonte cochlear,* among others, together with fossilized shells of *Modiolus modiolus* and debris of scleractinian corals (e.g., *Caryophyllia*) (Appendix A). Three cores were taken from this mound field with one core (TG22) collected from the top of a mound revealing a very low recovery of ~5–38 cm and only containing rhodoliths, while the two gravity cores (TG23-24) collected from the seabed adjacent to the Málaga mounds yielded core recoveries of more than 2 m only containing soft muddy sediments (Appendix A).

The bottom sediments and benthic and demersal communities of the Málaga mound field were similar to the ones detected in the Alcántara mound field, and included bathyal muds with burrowing megafauna (mainly *Munida* spp.), intermixed with seapens (mainly *V. cynomorium* and *Virgularia mirabilis*) and soft octocorals (*Alcyonum palmatum*), together with cerianthiids (*Cerianthus* spp.) and sabellid polychaetes (*Sabella pavonina*) (Dive 4; Dive 6) (Figures 4 and 5). Other benthic organisms detected were the hydrozoan *N. ramosa* and the soft bottom gorgonian *Spinimuricea* sp., the polychate *Spiochaetopterus* sp., decapods (*Dardanus arrosor, Monodaeus couchii, Macropodia* sp. and *Plesionika* spp.) as well as the gastropod *Xenophora crispa* and cephalopods (*Illexcoindetti*). Common fishes in this field are also similar to the ones detected in the Alcántara mound field and included unidentified species of Myctophids, the horse mackerel *Trachurus* spp., the dogfish *S. canicula*, small gobiids (*Lesueurigobius* spp.) and the monk fish *Lophius* sp. The fossil record included remains of solitary (mainly *Caryophyllia* spp.) and colonial scleractinians (*Dendrophyllia cornigera*), abundant remains of fossilized rhodoliths and of some bivalves (mainly *Glycymeris glycymeris* and *Modiolus modiolus*) (Figures 4 and 5). Bottom-trawling marks in this mound field represent human activities.

4.3. Aceitunas Mound Field

The Aceitunas mound field in the east has the largest extension and is located 10.5 km off Almería (north-westwards of Chella Bank), between 155 and 401 m water depth (Figures 1D and 2C). It is the most heterogeneous field and is composed of 243 mounds (Table 2). Most mounds have circular to subcircular shapes, but few of them have also elongated shapes (Iri > 1.8) showing a NW-SE orientation (Table 2). The mounds have heights up to 15 m and diameters between 6 to 630 m (Table 2), with maximum slopes of 20°. The mounds with steep flanks are located at the base of Chella Bank, developed on the flank of the rim depression surrounding the seamount (Figure 2C). In general, the circular mounds of this field are smaller (mean diameters: 123 m) and are generally located deeper (224 to 366 m) compared to the elongated mounds (lengths: 280 to 630 m; water depth: below 210 m). In the Aceitunas mound field, the distribution of the individual mounds follows a scallop pattern, with the largest mounds located at the western sector of

the field (with a mound density of 18 mounds per km^2) and the smallest ones located in the easternmost sector (with mound densities between one and five mounds per km^2).

The sediment surface samples VV09-21 were collected from different mounds in the Aceitunas mound field and consisted of fine muddy bioclastic sand with some pebbles, including some remains of bivalves and polychaetes. At the northernmost part of the Aceitunas mound field, the sediment contains more sand, showing diverse bioclastic fragments. Six gravity cores (TG16-21, with recoveries of 2 to 30 cm) retrieved from the top and flanks of the mounds of the Aceitunas field are characterized by bioclastic muddy sands, with some fragments of scleractinian corals (i.e., *Caryophyllia* spp.) (Appendix A).

In the Aceitunas mound field, the main bottom sediments were bathyal sandy muds and muddy sands and benthic and demersal communities were dominated by burrowing megafauna (mainly *Munida* spp.), intermixed with seapens (mainly *V. cynomorium* and *Virgularia mirabilis*) and octocorals (*Alcyonumpalmatum*), as well as with cerianthids (*Cerianthus* sp.) (Dive 7). Other benthic organisms include unidentified hydrozoans, decapods (*Dardanus* sp. and *Plesionika* spp.) as well as the gastropod *Xenophora crispa*. Common fishes in this field are also similar to the ones detected in the Alcántara and Málaga mound fields and included unidentified species of flatfishes and gobiids, the dogfish *S. canicula* and the blackbelly rosefish *Helicolenus dactylopterus*. In some mounds, remains of rhodoliths and of the seagrass *Posidonia oceanica* were commonly observed on the underwater images and were also detected in the collected sediment samples. Anthropic activity indicators were represented by several bottom-trawling marks, some of them being very well defined, as well as by remains of plastics and fabrics.

4.4. Subseafloor Features and Seismic Facies of the Mound Fields

The high-resolution seismic profiles revealed that the mounds are embedded in the Quaternary contouritic terrace deposits of the northern Alboran Sea margin. These deposits are made up of the vertical stacking of seaward tilted subparallel stratified facies with reflections of variable acoustic amplitude. These deposits show seismic discontinuities of wide lateral continuity that represent irregular erosive surfaces outstanding by their high acoustic reflectivity (Figure 3). These unconformities are sharp surfaces and are locally covered by an extensive (<80 km long) but thin (few millisecond (ms) thick) layers of transparent and chaotic reflections, whose top forms a surface of high reflectivity with irregular morphology. Locally, terrace deposits are affected by some ancient faults (Late Pleistocene in age, [77] that in the Alcántara mound field are sealed by the most recent erosive surface (Figure 3A).

The seismic sections of the mounds protruding at the seafloor show conical shapes with two main types of morphologies: single mounds with gently inclined flanks and clusters of mounds of different heights. Their basal parts are >300 m to <2 km long, with total heights varying from >5 to about 30 ms. These mounds root on at least three different erosive surfaces (i.e., with different ages; named lower, middle and upper in Figure 3). The transparent and chaotic level overlying the lower erosive surface resembles levels of similar, but much smaller within the mounds (Figure 3B). Some mounds continued to form since their initiation at the lower erosive surface, while others disappeared and new ones formed at the middle and upper erosive surfaces. The hummocky level overlying the lower erosive surface resembles levels of similar, but much smaller mounds due to their facies and morphology (Figure 3B). This suggests that the larger mounds build up as isolated features rooted on the erosive surfaces and also grew on extensive patches with multiple smaller mounds where locally, prominent mounds stand out and eventually protrude at the seafloor. In both cases, below the prominent mounds, acoustic anomalies, such as velocity pull-up (Figure 3B) and column-shaped blanking that mask completely or partially the underlying deposits (Figure 3) are observed. The mounds rooted on the most ancient surface are commonly those with the highest dimensions.

In general, the irregular topography created by the mounds elevating from the seafloor is infilled by stratified deposits (Figure 3). Their reflections seem to continue along the

sides of the mounds suggesting that most of them are at least covered by a variable thin (a few meters) layer of recent sediments. The mounds are internally defined by transparent facies. High reflectivity internal surfaces, vertically and laterally stacked are identified in some single cases. In the mound clusters, those surfaces are grouped with complex patterns (Figure 3B, C). Mounds with asymmetric cross sections are characterized by a relatively longer and steeper side with prolonged echoes, and a gentler flank showing wedges of stratified deposits at their foot (Figure 3A). Additionally, at the basal part of some Alcántara mounds, contourite moats (tens of meters wide, few ms in height) or moat-drift systems (few hundred meters in length) could be identified (Figure 3A).

Mounds are not exclusively found on the present seafloor. Seismic profiles from the Alcántara and Málaga mound fields show buried features similar in morphology and dimensions to the seafloor mounds (Figure 3B), pointing to additional, older mound formation periods. These older buried mounds and their surrounding contouritic sediments appear seismically very similar to the younger ones and, thus, indicate that mounds have been developed intermittently in the same areas during a long time period. The buried mounds also root on (at least up to 4) erosive surfaces (Figure 3B). The Alcántara and Aceitunas fields comprise 26 to 58 identified buried mounds, respectively, whilst in the Málaga field, more than 120 buried mounds are identified, which may represent the most ancient ones as some of them root on the deepest erosive surface (Figure 3).

5. Discussion

5.1. Potential Main Framework-Building Organisms of the Mounds

The present study could not confirm which framework-building organisms induced the formation and further development of the mounds of the northern Alboran Sea, but samples collected in the mound fields included remains of solitary and colonial scleractinians (e.g., *Caryophyllia* spp., *Dendrophyllia cornigera*), rhodoliths and large bivalves, with subordinate organisms. Organisms inducing mound formation generally include different groups with different biological traits, ranging from cyanobacteria and calcareous algae (mostly in mounds built in photic areas during ancient times) to heterozoans (mostly colonial scleractinians) without photoautotrophic symbionts (during past and modern times) but dependent on external food particles transported by bottom currents [2,4,5,26,30,33,78]. The morphologies and internal structures of the studied mounds in the northern Alboran Sea are similar to those reported for mounds detected in the southern Alboran Sea (East and West Melilla CWC mound Provinces) [43,46,55,61]. These southern Alboran Sea mounds are clear examples of carbonate mounds built by framework forming cold-water corals (CWCs) (mainly *Madrepora oculata* and *Desmophyllum pertusum*, the latter known as *Lophelia pertusa* until [79], so it is likely that CWCs could represent the dominating contributors for mound development in the northern Alboran Sea mounds. CWC mounds, either active (covered by thriving CWC reefs) or buried in soft sediments have been previously reported from many parts of the Mediterranean Sea (e.g., Apulian margin in the Ionian Sea -Santa Maria di Leuca CWC province, Corsica Channel-Tuscan Archipelago slope) [17,80–85] and the adjacent Gulf of Cádiz (e.g., [7,85–89]). Seismostratigraphic analysis and radiometric dating suggested that some of these mounds (e.g., EMP, WMP) experienced their most recent formation period during the last deglaciation until the Early Holocene most likely related to enhanced marine productivity [43] while older mound formation periods are placed (e.g., during the last interglacial [63]. The demise and subsequent burial of some Mediterranean CWC mounds since the Early to Mid-Holocene generally coincided with substantial changes in the environmental conditions driven by changes in climate water mass distribution [44,55,79,90], and water mass interfaces sculpting the regional contouritic erosive terraces [56]. These terraces have been created through time by turbulent oceanographic processes (e.g., internal waves) related to the water mass interfaces, and their vertical and lateral variations during the Late Quaternary sea-level variations [56,91].

In this sense, some southern Alboran Sea CWC mounds (e.g., WMP) significantly slowed down their aggradation during the Mid-Holocene due to relatively weak hydrody-

namics and oligotrophic conditions and, finally, stagnated until today with some mounds becoming buried and/or partially buried by sediments [46]. This contrasts with the high proliferation and aggradation rates of the southern Alboran Sea CWC mounds during the Bølling–Allerød interval, possibly related to enhanced surface ocean productivity and a peak in meltwater discharge originating from the northern Mediterranean borderlands, which caused a major reorganization of the Mediterranean thermohaline circulation [43,75]. Indeed, significant environmental changes on the continental slope decrease onshore sediment inputs to the continental slope due to landward migration of the coastline [6,92,93]. Hence, the mounds could be controlled by changes in the sediment focusing, resulting in lateral sediment supply and changing deposition on the mounds, as supported in [53] and also changes in the current bottom-current regimes. Considering all these observations, it is possible that changes in the water mass circulation and water column structure, productivity, near-bottom currents and sediment supply may also have induced the demise of the studied northern Alboran Sea mounds as detected in the southern Alboran Sea CWC mounds.

The studied carbonate mounds from the northern Alboran Sea are mostly buried by mud and muddy sands, over a thick layer of calcareous algae (mainly rhodoliths), with subordinate remains of solitary and colonial scleractinian (e.g., *Dendrophyllia cornigera*) and bivalve shells, including the horse mussels (*Modiolus modiolus*). In fact, several gravity cores were recovered from the mounds but they could just retrieve a maximum length of 38 cm of sediment, with the lowest 5 cm section of the cores containing rhodoliths, while gravity cores collected from the adjacent seabed only recovered soft sediments. Rhodolith beds occur commonly in the photic and mesophotic zones, generally at less than ca. 40 m water depth in the NE Atlantic and above ca. 120 m in the Mediterranean Sea in different coastal and offshore environmental settings [16,94]. Rhodolith beds can display considerable variation in thickness, with thicker beds occurring in settings with strong hydrodynamics [14]. In these settings, rhodolith beds can even display wave ripples or mega ripples (e.g., in Galway Bay, Stravanan Bay) [95,96]. In low energy settings, rhodoliths can conform minireefs made of the fusion of rhodoliths with other sessile organisms (e.g., Fernando de Noronha Island, Rocas Atol, Vitoria Trindade Chain, Brazil) [97,98]. Furthermore, some mobile organisms (e.g., the tilefish *Malacanthus plumieri*) can create small mounds of rhodoliths [97,98]. Nevertheless, no records of large mounds built by rhodoliths have been found in the literature, thus, it is more plausible that the rhodoliths developed just on top of the already existing carbonate mounds and, therefore, contributed to a minor extent to their aggradation. Rhodolith beds occur nowadays in the Alboran Sea (20–120 m) on the summits of Chella Bank (75–120 m) and of the Alboran ridge (20–100 m) [99,100]. Considering that rhodoliths may have been formed on top of the carbonate mounds when sea level was minimal during the Last Glacial because some of the studied carbonate mounds were located at suitable depth for rhodolith growth (ca. 53–110 m) during that period (Appendix A).

Together with the rhodoliths, remains of horse mussels (*M. modiolus*) were collected in some surface samples and were also detected in some underwater ROV images from the Málaga mound field. Graveyards of this mytilid have been found in other parts of the Alboran Sea, mainly at Chella Bank [96] and at the Alboran ridge (between 100–120 m) [99]. Graveyards of other mytilids have been detected in upper Miocene out cropped carbonates in a NE–SW trending belt (42 km long and 1.5–8 km wide) along the so-called El Alcor topographic high (Guadalquivir Basin, S Spain) [101]. In the *M. modiolus* graveyards of the Alboran Sea, remains of other bivalve species were detected, including *Panomya norvegica* and large individuals of *Mytilus edulis* [99]. The former species, together with *M. modiolus*, represent examples of boreal guests that occurred in the Alboran Sea during the Last Glacial, while today the distribution of these species is restricted to latitudes north of the English Channel in the NE Atlantic. A study [102] indicated that *M. modiolus* occurred intermittently in the Western Mediterranean Sea and adjacent Gulf of Cádiz from the late Pleistocene until the substantial warming accompanying Termination 1 of the Last Glacial

(ca. 13,000 years B.P.). Individuals of *M. modiolus* are best described as being adapted to live semi-infaunally with endobyssate attachment to the substrate, which ranges from soft or coarse sediments to rhodolith beds and hard substrata [103–105]. Generally, *M. modiolus* can be found on the lower shore in rock pools or in laminarian holdfasts but more common subtidally down to ca. 280 m depth [105]. This bivalve occurs singularly, in clumps, or in high-density and species-rich biogenic reefs in boreal and temperate regions around the world [106,107]. Some of the *M. modiolus* beds can extend ca. 349 ha (e.g., The North Lleyn reef, in the UK) and display undulating reliefs up to 1–2 m high, which are generally orientated perpendicular to the current [108]. Considering this, it is very unlikely that the carbonate mounds of the northern Alboran Sea, with heights of up to 18 m, would have been built up solely by the aggradation of *M. modiolus* beds, which generally are less than 2 m high, and no records of large mounds formed by this mytilid have been found in the literature. So, it is likely that these bivalves lived on top of some carbonate mounds together with the rhodoliths before they declined during Termination 1a of the Last Glacial, in accordance with [102].

5.2. Carbonate Mound Location and Environmental Setting

A large number of mound structures with acoustically transparent features presented in this study are interpreted as carbonate mounds, probably built by CWCs, considering the striking morphological and seismic similarities, such as their conical shape and the rooting on different seismic horizons, with other similar exposed and/or buried CWC mounds previously described in the Gulf of Cádiz [7,89], in the Porcupine Seabight [109,110] and in the southern Alboran Sea [55,61].

In general, larger and elongated mounds were detected in the shallowest areas whereas smaller mounds were detected in the deepest areas of the northern Alboran Sea mound fields. This is in accordance with the observations made by [55] for the WMP in the southern Alboran Sea, where smaller mounds were more frequent along the distal and deeper sectors of the mound field. The authors attributed this depth-related distribution pattern to a lower hydrodynamic energy setting and reduced food supply for CWCs in those deeper waters. Moreover, [46] detected stagnation of the southern Alboran Sea CWC mounds with the onset of the Mid Holocene, because they were located in an oligotrophic setting. This contrasts with the strong hydrodynamic setting promoted by internal waves developed along the water mass interface between the MAW and the LIW during the Bølling–Allerød (B/A) interstadial and the Early Holocene [46]. If water mass properties and internal waves (developed along the water mass interface) controlled the proliferation of CWCs and hence the development of CWC mounds, it is likely that the larger elongated mounds were more exposed to these internal waves with an efficient food delivery than the small mounds located deeper. Since for the northern and central Alboran Sea, the interval waves are currently reported from the interface between MAW and LIW at ~250 m water depth [111], the studied mounds, which occur in a relatively narrow depth range, should be influenced by internal waves in the same way. The elongated mounds located in the shallowest sectors of the studied fields could also have been benefitted more from food particles generated through the nutrient-rich coastal upwelling waters of the northern Alboran Sea [68]. Thus, the interaction between enhanced productivity and hydrodynamic energy settings in the shallowest areas probably has provided more suitable conditions for CWC growth and carbonate mound aggradation, allowing individual small mounds to merge to more complex structures conforming to larger, elongated CWC mounds as also found in other areas [112–114].

In the northern Alboran Sea, the carbonate mounds of the shallowest sectors are elongated with a predominant downslope extension of their length axis, mainly following NW-SE directions rather than parallel to the bathymetric contours of the continental slope. This probably might be related to the activity of internal waves developed along the water mass interface between the MAW and the LIW which could influence the shape and orientation of the mounds as assumed for carbonate mounds of the Gulf of Cádiz [7].

Furthermore, these internal waves and the generated strong hydrodynamic energy setting could also have played a big role in shaping the contourite terraces where the studied mound fields are located [56]. The sustained effect of a strong hydrodynamic energy setting, as observed by extended contourite deposition at several sites in the Alboran Sea [56,115], is clearly displayed in the present-day topography of the studied carbonate mound fields with many of the mounds being aligned by extensive moats, which are more pronounced around the Alcántara mounds, implying a more vigorous bottom current regime there (Figure 2A). This fact can be related to the constriction and acceleration of Mediterranean water masses near the Strait of Gibraltar [116].

The morphometric analysis of the studied carbonate mounds at the upper slope of the northern Alboran Sea revealed a total of 325 exposed carbonate mounds and 204 buried ones, extending over the three areas of almost 5.5 km^2 and resulting in a mean mound density of 62 mounds per km^2 for the northern Alboran Sea. In the Aceitunas mound field, the mean mound density reaches up to 78 mounds per km^2, hence being much larger than in the Málaga and Alcántara mound fields (Figure 2D–F). Such mound densities are much higher than the ones detected for other CWC mound fields from the Mediterranean Sea, with 3–5 mounds per km^2 were observed [55], and from the Moroccan margin, with 2–12 mounds per km^2 [89,117]. The high number of carbonate mounds observed for various mound provinces in the Atlantic and Mediterranean [4,7,8,50,81,118], and now, in the Alboran Sea, point to their role as common seafloor morphological features usually occurring in intermediate water depths, which should be considered for future seafloor classification studies.

Furthermore, the high-resolution seismic investigations provide evidence that striking regional and high acoustic amplitude erosional surfaces represent the base of the mounds, as has been also observed in the Gulf of Cádiz [88]. Based on seismic stratigraphy works using high-resolution seismic profiles in the Alboran Sea, we can tentatively suggest that those surfaces formed from latest Pleistocene to Holocene [56,93,119]. Their formation would have formed during phases of erosion shaping the contouritic terrace and during periods of relatively higher energetic bottom currents, related with climatic variability [56]. Consequently, these erosional surfaces likely provided hard substrates (e.g., lag deposits) that could have allowed initial colonization by CWC and subsequent reef formation, favored by topography-enhanced bottom currents.

5.3. Current and Past Sedimentary Environment Affecting the Mound Fields

Nowadays, the studied carbonate mounds can be considered inactive mound fields with no living CWCs and with most of the mounds buried in soft sediments as detected in other carbonate mounds of the NE Atlantic and Mediterranean Sea [33,55,120]. The associated communities in all three fields are very similar regarding their megafauna, mainly due to the fact that there are no extreme changes in the sediment type and depth among them, which generally represent two of the most important factors inducing species replacements in megabenthic communities. The detected megabenthic communities are very widespread in the northern Alboran Sea and are often exposed to bottom trawling activities because they attract valuable commercial fisheries resources [72]. Indeed, several trawling marks were detected in the underwater images obtained from the studied carbonate mounds. The bottom sediments and associated benthic communities on the mounds are similar to those detected on the seafloor adjacent to the mounds, indicating a very low present-day benthic heterogeneity between the studied mounds and the surrounding seabed. Generally, mound formation requires mound growth to be faster than background sedimentation, and baffling of hemipelagic sediment is a major component contributing to mound growth (especially in branching mound-forming organisms; [5,18,20,33,34,53]. Thus, the burial of carbonate mounds appears to be a consequence of the cessation of active reefs and, thus, mound growth induced by the deterioration of living conditions for the respective mound-forming organisms [5]. In the southern Alboran Sea, stagnation in mound formation occurred since the Mid-Holocene and some of these mounds became

buried by sediments. In the present study, it is not possible to place the development of the northern Alboran Sea mounds into any temporal framework or know precisely when the burial of the mounds took place. The burial induced extreme changes in the seabed and associated communities, from complex and highly diverse CWC and rhodolith bed communities, which probably formed since/during the Last Glacial Maximum, to current soft sediments with burrowing organisms and the specialized soft-bottom suspension feeders of the typical bathyal communities of the northern Alboran Sea [17].

The arrangements of the three erosive surfaces observed in the sub-bottom profiles (Figure 3), as well as on the stratigraphic relationships between the buried mounds and the stratification of the sedimentary deposits allow us to conclude that active sedimentation generated stratified deposits overlying the carbonate mounds. Laterally, the continuity of the deposits seems to be interrupted by the mounds themselves, once they are inactive. This suggests that the mounds were formed shortly after the major erosional event that created the hardground mound base common for the three fields and developed quickly, likely promoted by favorable oceanographic and climatic conditions, before strong drift sedimentation started [109]. Such mound-controlled processes have already been suggested for other CWC mound provinces off Ireland [113,120]. The inferred age of the lower rooted surface at the base of the mounds is late Pliocene to early Quaternary, so the stage of formation of the mounds would date from the early Quaternary.

6. Conclusions

Based on these observations, we consider that the occurrence pattern of the northern Alboran Sea mounds could be related to favorable climatic conditions for CWC mound formation, possibly during the Quaternary and before Termination 1a of the Last Glacial due to the occurrence of boreal guest fauna on top of the mounds. This contrasts with the findings of [15,43,46] who detected that the most recent mound formation period started during the last deglaciation in some southern Alboran Sea mounds (e.g., WMP). Although direct observation of the typical CWCs involved in mound formation (e.g., *Madrepora oculata, Desmophyllum pertusum*) could not be carried out in the present study, it is very plausible that CWCs represented the main mound-building organisms due to the morphological similarities and internal structure of the studied mounds. Further studies may focus on obtaining long cores using extracting methods (e.g., drilling) that are more efficient than gravity coring in order to improve the knowledge on the internal composition of the mounds as well as in performing seismostratigraphic analyses and radiocarbon dating of the rhodolith outer surface. In addition, bathymetry and high-resolution seismic profiles could be obtained with equipment operating closer to the seafloor, such as autonomous underwater vehicles (AUVs). This would allow us to obtain detailed bathymetry, backscatter and seismic profiles to study the internal structure of the mounds and to correlate their morphostructure with long sediment corers in order to advance the knowledge of the formation and evolution of the northern Alboran Sea mounds.

Author Contributions: Conceptualization, O.S.-G., M.G.-B. and J.L.R.; Funding acquisition, M.G.-B., G.E., C.W. and D.H.; Methodology, O.S.-G., M.G.-B., J.L.R., J.U. and J.T.V.; Species identification, J.L.R., J.U., E.M.-U., C.W. and D.H.; Formal analysis, O.S.-G., J.L.R., C.W., D.H., M.G.-B., J.T.V., F.E. and G.E.; Data curation, All authors; Writing—original draft, review & editing, All authors; Supervision, O.S.-G., J.L.R., C.W. and D.H. All authors have read and agreed to the published version of the manuscript.

Funding: This research was performed in the scope of MONCARAL and RIGEL projects, funded by the Instituto Español de Oceanografía (IEO), and the AGORA project (P18-RT-3275) (funded by Junta de Andalucía).

Institutional Review Board Statement: Not applicable.

Informed Consent Statement: Not applicable.

Data Availability Statement: Datasets are stored in the database of the Instituto Español de Oceanografía (IEO) for the MONCARAL and RIGEL projects, some of which is available at the IEO marine geospatial information viewers and services: http://www.ieo.es/en/ideo (accessed on 15 December 2021).

Acknowledgments: This work is a contribution from "Contraste de la actividad geológica entre el sector este y oeste del mar de Alborán y cordilleras adyacentes": AGORA (*P18-RT-3275* (Junta de Andalucía), "Estudio y caracterización de montículos carbonatados en el Mar de Alborán": MONCARAL (IEO) funded projects as well to a contribution of the ESMARES 2 (MITERD and Instituto Español de Oceanografía) project for improving the knowledge on the circalitoral and bathyal habitats of the northern Alboran Sea (Demarcación Estrecho-Alboran) (18ESMARES2-CIRCA). We appreciate all the valuable help made by the captains, crews and scientific teams during the POS-385, MONCARAL 0516 and RIGEL 1116 expeditions on board R/V Poseidon and R/V Ángeles Alvariño. This work acknowledges to the 'Severo Ochoa of Excellence'accreditation (*CEX2019-000928-S*).

Conflicts of Interest: The authors declare any conflict of interest.

Appendix A

Table A1. Metadata of the surface sediment Van veen grab samples (VV) and gravity cores (TG) recovered during MONCARAL_0516 and RIGEL_1116 expeditions in the northern Alboran Sea.

Expedition	Mound Field	Sample Code	Core Length (cm)	Water Depth (m)	Latitude N (°)	Longitude W (°)	Description
MONCARAL	Alcántara	VV01		241	36°21.52′	05°01.40′	Muddy sand with *Nucula sulcata* and *Nassarius ovoideus* shells
MONCARAL	Alcántara	VV02		251	36°21.36′	05°01.45′	Muddy sand with *Nucula sulcata* and *Euspira fusca* shells
MONCARAL	Alcántara	VV03		317	36°19.83′	04°59.86′	Sandy mud with *Abra* spp. and *Nassarius ovoideus*
MONCARAL	Alcántara	VV04		313	36°19.85′	04°59.80′	Muddy sand
MONCARAL	Málaga	VV05		231	36°37.70′	04°12.90′	Bioclastic sandy mud with rhodoliths and *Modiolus modiolus* shells fragments
MONCARAL	Málaga	VV06		260	36°37.20′	04°12.10′	Bioclastic sandy mud with *Neopycnodonte cochlear* shells and *Caryophyllia* spp. fragments
MONCARAL	Málaga	VV07/08		271	36°37.01′	04°11.60′	Sandy mud with *Nassarius ovoideus* and *Aporrhais serresiana* shells
MONCARAL	Aceitunas	VV09		192	36°36.50′	02°54.50′	Muddy fine sand with *Posidonia oceanica* remains
MONCARAL	Aceitunas	VV10		201	36°36.20′	02°54.30′	Bioclastic sand with rhodoliths fragments
MONCARAL	Aceitunas	VV11		173	36°37.00′	02°56.20′	Bioclastic sand with rhodoliths fragments
RIGEL	Aceitunas	VV16		223	36°36.37′	2°56.61′	Bioclastic muddy sand
RIGEL	Aceitunas	VV17		233	36°35.36′	2°53.61′	Bioclastic muddy sand with *Caryophyllia* spp. fragments
RIGEL	Aceitunas	VV18		244	36°35.14′	2°52.79′	Sandy mud
RIGEL	Aceitunas	VV19		188	36°36.20′	2°53.48′	Sandy mud
RIGEL	Aceitunas	VV20		196	36°36.31′	2°54.88′	Sandy mud
RIGEL	Aceitunas	VV21		231	36°38.52′	4°10.16′	Sandy mud
RIGEL	Málaga	VV22		238	36°37.66′	4°11.94′	Bioclastic sandy mud
RIGEL	Málaga	VV23		255	36°37.59′	4°11.17′	Sandy mud with polychaetes
RIGEL	Málaga	VV24		232	36°37.82′	4°12.85′	Sandy mud
RIGEL	Aceitunas	TG16	7	171	36°37.04′	2°56.18′	Bioclastic muddy sand
RIGEL	Aceitunas	TG17	5	172	36°37.05′	2°56.19′	Bioclastic muddy sand
RIGEL	Aceitunas	TG18	30	191	36°36.25′	2°54.46′	Bioclastic muddy sand
RIGEL	Aceitunas	TG19	5	194	36°36.19′	2°54.38′	Bioclastic muddy sand with *Caryophyllia* spp. fragments
RIGEL	Aceitunas	TG20	26	193	36°36.38′	2°54.78′	Bioclastic muddy sand with *Caryophyllia* spp. fragments
RIGEL	Aceitunas	TG21	2	233	36°35.36′	2°53.61′	Bioclastic sandy mud
RIGEL	Málaga	TG22	38	231	36°38.52′	4°10.16′	Sandy mud with *N. cochlear* shells fragments and rhodoliths
RIGEL	Málaga	TG23	260	248	36°37.34′	4°12.12′	Bioclastic sandy mud
RIGEL	Málaga	TG24	105	231	36°37.82′	4°12.85′	Bioclastic sandy mud

References

1. Mienis, F.; van Weering, T.; Haas, H.; Stigter, H.; Huvenne, V.; Wheeler, A. Carbonate Mound Development at the SW Rockall Trough Margin Based on High Resolution TOBI and Seismic Recording. *Mar. Geol.* **2006**, *233*, 1–19. [CrossRef]
2. Monty, C.L.V.; Bosence, D.W.J.; Bridges, P.H.; Pratt, B.R. Carbonate Mud-Mounds Their Origin and Evolution. In *International Association of Sedimentologists*; Special Publication 23; Blackwell Science Ltd.: Oxford, UK, 1995; p. 537.

3. International Hydrographic Organization. Standardization of undersea feature names. In *Guidelines Proposal Form Terminology*; English/Spanish Version Edition 4.1.0; Bathymetric Publication No. 6; International Hydrographic Bureau: Monte Carlo, Monaco, 2013.
4. Henriet, J.P.; Hamoumi, N.; Da Silva, A.C.; Foubert, A.; Lauridsen, B.W.; Rüggeberg, A.; Van Rooij, D. Carbonate Mounds: From Paradox to World Heritage. *Mar. Geol.* **2014**, *352*, 89–110. [CrossRef]
5. Hebbeln, D.; Samankassou, E. Where Did Ancient Carbonate Mounds Grow—In Bathyal Depths or in Shallow Shelf Waters? *Earth-Sci. Rev.* **2015**, *145*, 56–65. [CrossRef]
6. Ercilla, G.; Casas, D.; Alonso, B.; Casalbore, D.; Estrada, F.; Idárraga-García, J.; López-González, N.; Pedrosa, M.; Teixeira, M.; Sánchez-Guillamón, O.; et al. Deep Sea Sedimentation. *Ref. Modul. Earth Syst. Environ. Sci.* 2021. [CrossRef]
7. Hebbeln, D.; Bender, M.; Gaide, S.; Titschack, J.; Vandorpe, T.; Rooij, D.; Wintersteller, P.; Wienberg, C. Thousands of Cold-Water Coral Mounds along the Moroccan Atlantic Continental MargIn Distribution and Morphometry. *Mar. Geol.* **2019**, 411. [CrossRef]
8. Tamborrino, L.; Wienberg, C.; Titschack, J.; Wintersteller, P.; Mienis, F.; Schröder-Ritzrau, A.; Freiwald, A.; Orejas, C.; Dullo, W.-C.; Haberkern, J.; et al. Mid-Holocene extinction of cold-water corals on the Namibian shelf steered by the Benguela oxygen minimum zone. *Geology* **2019**, *47*, 1185–1188. [CrossRef]
9. Freiwald, A.; Henrich, R.; Pätzold, J. Anatomy of a deep-water coral reef from Stjernsund, West Finmark, Northern Norway. In *Cool-Water Carbonates*; James, N.P., Clarke, J.A.D., Eds.; Special Publications—SEPM: Broken Arrow, OK, USA, 1997; Volume 56, pp. 141–162.
10. Roberts, J.M.; Wheeler, A.; Freiwald, A. Reefs of the Deep: The Biology and Geology of Cold-Water Coral Ecosystems. *Science* **2006**, *312*, 543–547. [CrossRef]
11. Conway, K.; Krautter, M.; Barrie, J.; Whitney, F.; Thomson, R.; Reiswig, H.; Lehnert, H.; Mungov, G.; Bertram, M. Sponge Reefs in the Queen Charlotte Basin, Canada: Controls on Distribution, Growth and Development. In *Cold-Water Corals and Ecosystems*; Freiwald, A., Roberts, J.M., Eds.; Springer: Berlin/Heidelberg, Germany, 2005; pp. 605–621. [CrossRef]
12. Georgieva, M.N.; Paull, C.K.; Little, C.T.S.; McGann, M.; Sahy, D.; Condon, D.; Lundsten, L.; Pewsey, J.; Caress, D.W.; Vrijenhoek, R.C. Discovery of an Extensive Deep-Sea Fossil Serpulid Reef Associated with a Cold Seep, Santa Monica Basin, California. *Front. Mar. Sci.* **2019**, *6*, 115. [CrossRef]
13. James, N.; Feary, D.; Surlyk, F.; Simo, T.; Betzler, C.; Holbourn, A.; Li, Q.; Matsuda, H.; Machiyama, H.; Brooks, G.; et al. Quaternary Bryozoan Reef Mounds in Cool-Water, Upper Slope Environments: Great Australian Bight. *Geology* **2000**, 28. [CrossRef]
14. Mortensen, P.; Buhl-Mortensen, L.; Dolan, M.; Dannheim, J.; Kröger, K. Megafaunal diversity associated with marine landscapes of northern Norway: A preliminary assessment. *Nor. J. Geol.* **2009**, *89*, 163–171.
15. Stalder, C.; Vertino, A.; Rosso, A.; Rüggeberg, A.; Pirkenseer, C.; Spangenberg, J.E.; Spezzaferri, S.; Camozzi, O.; Rappo, S.; Hajdas, I. Microfossils, a Key to Unravel Cold-Water Carbonate Mound Evolution through Time: Evidence from the Eastern Alboran Sea. *PLoS ONE* **2015**, *10*, e0140223. [CrossRef] [PubMed]
16. Riosmena-Rodríguez, R.; Nelson, W.; Aguirre, J. Rhodolith/Maërl Beds: A Global Perspective. In *Coastal Research Library*; Springer: Cham, Switzerland, 2017; Volume 15. [CrossRef]
17. Rueda, J.L.; Urra, J.; Aguilar, R.; Angeletti, L.; Bo, M.; García-Ruiz, C.; González-Duarte, M.M.; López, E.; Madurell, T.; Maldonado, M.; et al. Cold-water coral associated fauna in the Mediterranean Sea and adjacent areas. In *Mediterranean Cold-Water Corals: Past, Present and Future. Coral Reefs of the World 9*; Orejas, C., Jiménez, C., Eds.; Springer International Publishing AG, part of Springer Nature: Berlin, Germany, 2019; pp. 295–333. [CrossRef]
18. Hebbeln, D.; Van Rooij, D.; Wienberg, C. Good neighbours shaped by vigorous currents: Cold-water coral mounds and contourites in the North Atlantic. *Mar. Geol.* **2016**, *378*, 171–185. [CrossRef]
19. Riding, R. Structure and Composition of Organic Reefs and Carbonate Mud Mounds: Concepts and Categories. *Earth. Sci. Rev.* **2002**, *58*, 163–231. [CrossRef]
20. Roberts, J.M.; Wheeler, A.; Freiwald, A.; Cairns Stephen, D. *Cold-Water Corals: The Biology and Geology of Deep-Sea Coral Habitats*; Cambridge University Press: Cambridge, UK, 2009.
21. Dullo, W.-C.; Flögel, S.; Rüggeberg, A. Cold-Water Coral Growth in Relation to the Hydrography of the Celtic and Nordic European Continental Margin. *Mar. Ecol. Prog. Ser.* **2008**, *371*, 165–176. [CrossRef]
22. Davies, A.J.; Guinotte, J.M. Global Habitat Suitability for Framework-Forming Cold-Water Corals. *PLoS ONE* **2011**, *6*, e18483. [CrossRef] [PubMed]
23. Thresher, R.E.; Tibrook, B.; Fallon, S.; Wilson, N.C.; Adkins, J.F. Effects of chronic low carbonate saturation levels on the distribution, growth and skeletal chemistry of deep-sea corals and other seamount megabenthos. *Mar. Ecol. Prog. Ser.* **2011**, *442*, 87–99. [CrossRef]
24. Wienberg, C.; Titschack, J. Framework-forming scleractinian cold-water corals through space and time: A late Quaternary North Atlantic perspective. In *Marine Animal Forests: The Ecology of Benthic Biodiversity Hotspots*; Rossi, S., Bramanti, L., Gori, A., Orejas, C., Eds.; Springer: Cham, Switzerland, 2017; pp. 699–732. [CrossRef]
25. Puerta, P.; Johnson, C.; Carreiro-Silva, M.; Henry, L.-A.; Kenchington, E.; Morato, T.; Kazanidis, G.; Rueda, J.L.; Urra, J.; Ross, S.; et al. Influence of Water Masses on the Biodiversity and Biogeography of Deep-Sea Benthic Ecosystems in the North Atlantic. *Front. Mar. Sci.* **2020**, *7*, 239. [CrossRef]

26. White, M.; Mohn, C.; de Stigter, H.; Mottram, G. Deep-water coral development asa function of hydrodynamics and surface-productivity around the submarine banks ofthe Rockall Trough, NE Atlantic. In *Cold-Water Corals and Ecosystems*; Freiwald, A., Roberts, J.M., Eds.; Springer: Berlin/Heidelberg, Germany, 2005; pp. 503–514.
27. Mienis, F.; de Stigter, H.C.; White, M.; Duineveld, G.; de Haas, H.; van Weering, T.C.E. Hydrodynamic Controls on Cold Water Coral Growth and Carbonate Mound Development at the SW and SE Rockall Trough Margin, NE Atlantic Ocean. *Deep. Res. Part 1. Oceanogr. Res. Pap.* **2007**, *54*, 1655–1674. [CrossRef]
28. Duineveld, G.; Lavaleye, M.; Bergman, M.; Stigter, H.; Mienis, F. Trophic Structure of a Cold-Water Coral Mound Community (Rockall Bank, NE Atlantic) in Relation to the near-Bottom Particle Supply and Current Regime. *Bull. Mar. Sci.* **2007**, *81*, 449–467.
29. Duineveld, G.C.A.; Jeffreys, R.M.; Lavaleye, M.S.S.; Davies, A.J.; Bergman, M.J.N.; Watmough, T.; Witbaard, R. Spatial and tidal variation in food supply to shallow cold-water coral reefs of theMingulay Reef complex (Outer Hebrides, Scotland). *Mar. Ecol. Prog. Ser.* **2012**, *444*, 97–115. [CrossRef]
30. Davies, A.J.; Duineveld, G.C.; Lavaleye, M.S.; Bergman, M.J.; van Haren, H.; Roberts, J.M. Downwelling and deep-water bottom currents as food supply mechanisms to the cold-water coral *Lophelia pertusa* (Scleractinia) at the Mingulay Reef complex. *Limnol. Oceanogr.* **2009**, *54*, 620–629. [CrossRef]
31. Taviani, M.; Angeletti, L.; Beuck, L.; Campiani, E.; Canese, S.; Foglini, F.; Freiwald, A.; Montagna, P.; Trincardi, F. On and off the Beaten Track: Megafaunal Sessile Life and Adriatic Cascading Processes. *Mar. Geol.* **2015**, *375*. [CrossRef]
32. Dorschel, B.; Hebbeln, D.; Rüggeberg, A.; Dullo, C. Carbonate Budget of a Cold-Water Coral Carbonate Mound: Propeller Mound, Porcupine Seabight. *Int. J. Earth Sci.* **2007**, *96*, 73–83. [CrossRef]
33. Mienis, F.; de Stigter, H.C.; de Haas, H.; van Weering, T.C.E. Near-bed perticle deposition and resuspention in a cold-water coral moundd area at the Southwest Rockall trough margin, NE Atlantic. *Deep-Sea Research Part 1* **2009**, *56*, 1026–1040. [CrossRef]
34. Fentimen, R.; Feenstra, E.; Rüggeberg, A.; Vennemann, T.; Hajdas, I.; Adatte, T.; Van Rooij, D.; Foubert, A. Cold-Water Coral Mound Archive Provides Unique Insights Into Intermediate Water Mass Dynamics in the Alboran Sea During the Last Deglaciation. *Front. Mar. Sci.* **2020**, *7*, 354. [CrossRef]
35. Dorschel, B.; Hebbeln, D.; Rüggeberg, A.; Dullo, W.-C.; Freiwald, A. Growth and Erosion of a Cold-Water Coral Covered Carbonate Mound in the Northeast Atlantic during the Late Pleistocene and Holocene. *Earth Planet. Sci. Lett.* **2005**, *233*, 33–44. [CrossRef]
36. Kano, A.; Ferdelman, T.G.; Williams, T.; Henriet, J.P.; Ishikawa, T.; Kawagoe, N.; Takashima, C.; Kakizaki, Y.; Abe, K.; Sakai, S.; et al. the IODP Exp. 307 Scientists. Age constraints on the origin and growth history of a deep-water coral mound in the northeast Atlantic drilled during Integrated Ocean Drilling Program Expedition 307. *Geology* **2007**, *35*, 1051–1054. [CrossRef]
37. Frank, N.; Freiwald, A.; López Correa, M.; Wienberg, C.; Eisele, M.; Hebbeln, D.; D, V.; JP, H.; Colin, C.; van Weering, T.; et al. Northeast Atlantic Cold-Water Coral Reefs and Climate. *Geology* **2011**, *39*, 743–746. [CrossRef]
38. Wienberg, C.; Frank, N.; Mertens, K.; Stuut, J.-B.; Marchant, M.; Fietzke, J.; Mienis, F.; Hebbeln, D. Glacial Cold-Water Coral Growth in the Gulf of Cádiz: Implications of Increased Palaeo-Productivity. *Earth Planet. Sci. Lett.* **2010**, *298*, 405–416. [CrossRef]
39. Thierens, M.; Browning, E.; Pirlet, H.; Loutre, M.F.; Dorschel, B.; Huvenne, V.A.I.; Titschack, J.; Colin, C.; Foubert, A.; Wheeler, A.J. Cold-Water Coral Carbonate Mounds as Unique Palaeo-Archives: The Plio-Pleistocene Challenger Mound Record (NE Atlantic). *Epic. Sci. Rev.* **2013**, *73*, 14–30. [CrossRef]
40. Freiwald, A.; Fosså, J.; Grehan, A.; Koslow, T.; Roberts, J. *Cold-Water Coral Reefs: Out of Sight—No Longer out of Mind*; UNEP-WCMC: Cambridge, UK, 2004.
41. Eisele, M.; Hebbeln, D.; Wienberg, C. Growth History of a Cold-Water Coral-Covered Carbonate Mound—Galway Mound, Porcupine Seabight, NE Atlantic. *Mar. Geol.* **2008**, *253*, 160–169. [CrossRef]
42. Fink, H.; Wienberg, C.; Hebbeln, D.; Mcgregor, H.; Schmiedl, G.; Taviani, M.; Freiwald, A. Oxygen Control on Holocene Cold-Water Coral Development in the Eastern Mediterranean Sea. *Deep Sea Res. Part I Oceanogr. Res. Pap.* **2012**, *62*, 89–96. [CrossRef]
43. Fink, H.G.; Wienberg, C.; De Pol-Holz, R.; Wintersteller, P.; Hebbeln, D. Cold-Water Coral Growth in the Alboran Sea Related to High Productivity during the Late Pleistocene and Holocene. *Mar. Geol.* **2013**, 71–82. [CrossRef]
44. Fink, H.G.; Wienberg, C.; De Pol-Holz, R.; Hebbeln, D. Spatio-temporal distribution patterns of Mediterranean cold-water corals (*Lophelia pertusa* and *Madrepora oculata*) during the past 14,000 years. *Deep-Sea Res. I Oceanogr. Res. Pap.* **2015**, *103*, 37–48. [CrossRef]
45. Van der Land, C.; Eisele, M.; Mienis, F.; de Haas, H.; Hebbeln, D.; Reijmer, J.J.G.; van Weering, T.C.E. Carbonate mound development in contrasting settings on the Irish margin. *Deep-Sea Res. Part 2 Top. Stud. Oceanogr.* **2014**, *99*, 297–306. [CrossRef]
46. Wang, H.; Lo Iacono, C.; Wienberg, C.; Titschack, J.; Hebbeln, D. Cold-Water Coral Mounds in the Southern Alboran Sea (Western Mediterranean Sea): Internal Waves as an Important Driver for Mound Formation since the Last Deglaciation. *Mar. Geol.* **2019**, *412*, 1–18. [CrossRef]
47. Cyr, F.; van Haren, H.; Mienis, F.; Duineveld, G.; Bourgault, D. On the Influence of Cold-Water Coral Mound Size on Flow Hydrodynamics, and Vice Versa. *Geophys. Res. Lett.* **2016**, *43*, 775–783. [CrossRef]
48. Mullins, H.T.; Newton, C.R.; Heath, K.; Van Buren, H.M. Modern deep-water coral mounds north of Little Bahama Bank: Criteria for the recognition of deep-water coral bioherms in the rock record. *J. Sediment. Petrol.* **1981**, *51*, 999–1013.

49. Kirkby, K.C.; Hunt, D. Episodic growth of a Waulsortian buildup: The Lower Carboniferous Muleshoe Mound, Sacramento Mountains, New Mexico, USA. In *Recent Advances in Lower Carboniferous Geology*; Strogen, P., Somerville, I.D., Jones, G.L., Eds.; Special Publications: London, UK, 1996; Volume 107, pp. 97–110.
50. De Mol, B.; Van Rensbergen, P.; Pillen, S.; Van Herreweghe, K.; Van Rooij, D.; Mc Donnell, A.; Huvenne, V.; Ivanov, M.; Swennen, R.; Henriet, J.P. Large deep-water coral banks in the Porcupine Basin, southwest of Ireland. *Mar. Geol.* **2002**, *188*, 193–231. [CrossRef]
51. Grasmueck, M.; Eberli, G.; Correa, T.; Viggiano, D.A.; Luo, J.; Wyatt, G.J.; Reed, J.; Wright, A.; Pomponi, S.A. AUV-Based Environmental Characterization of Deepwater Coral Mounds in the Straits of Florida. *OTC* **2007**, 158–169. [CrossRef]
52. Titschack, J.; Baum, D.; De Pol-Holz, R.; López Correa, M.; Forster, N.; Flögel, S.; Hebbeln, D.; Freiwald, A. Aggradation and Carbonate Accumulation of Holocene Norwegian Cold-Water Coral Reefs. *Sedimentology* **2015**, *62*, 1873–1898. [CrossRef]
53. Wang, H.; Titschack, J.; Wienberg, C.; Korpanty, C.; Hebbeln, D. The Importance of Ecological Accommodation Space and Sediment Supply for Cold-Water Coral Mound Formation, a Case Study From the Western Mediterranean Sea. *Front. Mar. Sci.* **2021**, *8*, 1941. [CrossRef]
54. Margreth, S.; Gennari, G.; Rüggeberg, A.; Comas, M.C.; Pinheiro, L.M.; Spezzaferri, S. Growth and demise of cold-water coral ecosystemson mud volcanoes in theWest Alboran Sea: The messages from the planktonic and benthic foraminifera. *Mar. Geol.* **2011**, *282*, 26–39. [CrossRef]
55. Lo Iacono, C.; Gràcia, E.; Ranero, C.R.; Emelianov, M.; Huvenne, V.; Bartolomé, R.; Booth-Rea, G.; Prades, J. The West Melilla Cold Water Coral Mounds, Eastern Alboran Sea: Morphological Characterization and Environmental Context. *Deep Sea Res. Part II Top. Stud. Oceanogr.* **2014**, *99*, 316–326. [CrossRef]
56. Ercilla, G.; Juan, C.; Estrada, F.; Alonso, B.; Casas, D.; Farran, M.; García, M.; Ammar, A. Significance of Bottom Currents in Deep-Sea Morphodynamics: An Example from the Alboran Sea. *Mar. Geol.* **2016**, *378*, 157–170. [CrossRef]
57. Juan, C.; Ercilla, G.; Estrada, F.; Alonso, B.; Casas, D.; Vázquez, J.T.; d'Acremont, E.; Medialdea, T.; Hernández-Molina, F.J.; Gorini, C.; et al. Multiple Factors Controlling the Deep Marine Sedimentation of the Alboran Sea (SW Mediterranean) after the Zanclean Atlantic Mega-Flood. *Mar. Geol.* **2020**, 423. [CrossRef]
58. Ballesteros, M.; Rivera, J.; Muñoz, A.; Muñoz-Martín, A.; Acosta Yepes, J.; Gorosabel, A.; Uchupi, E. Alboran Basin, Southern Spain. Part II: Neogene Tectonic Implications for the Orogenic Float Model. *Mar. Pet. Geol* **2008**, *25*. [CrossRef]
59. Pereiro-Muñoz, A.; Ballesteros, M.; Montoya, I.; Rivera, J.; Acosta, J.; Uchupi, E. Alborán Basin, southern Spain—Part I: Geomorphology. *Mar. Petrol. Geol.* **2008**, *25*, 59–73. [CrossRef]
60. Hebbeln, D. *Report and Preliminary Results of RV POSEIDON Cruise POS 385 "Cold-Water Corals of the Alboran Sea (Western Mediterranean Sea)", Faro—Toulon, May 29—June 16, 2009*; Universität Bremen: Bremen, Germany, 2009; pp. 1–79.
61. Hebbeln, D. Highly variable submarine landscapes in the Alborán Sea created by cold-water corals. In *Mediterranean Cold-Water Corals: Past, Present and Future: Understanding the Deep-Sea Realms of Coral*; Orejas, C., Jiménez, C., Eds.; Springer International Publishing: Cham, Switzerland, 2019; pp. 61–65.
62. Corbera, G.; Lo Iacono, C.; Gràcia, E.; Grinyó, J.; Pierdomenico, M.; Huvenne, V.A.I.; Aguilar, R.; Maria Gili, J. Ecological characterisation of a Mediterranean cold-water coral reef: Cabliers Coral Mound Province (Alboran Sea, western Mediterranean). *Prog. Oceanog.* **2019**, *175*, 245–262. [CrossRef]
63. Corbera, G.; Lo Iacono, C.; Standish, C.; Anagnostou, E.; Titschack, J.; Katsamenis, O.; Cacho, I.; Rooij, D.; Huvenne, V.; Foster, G. Glacio-Eustatic Variations and Sapropel Events as Main Controls on the Middle Pleistocene-Holocene Evolution of the Cabliers Coral Mound Province (W Mediterranean). *Quat. Sci. Rev.* **2021**, *253*. [CrossRef]
64. Lo Iacono, C.; Gràcia, E.; Diez, S.; Bozzano, G.; Moreno, X.; Dañobeitia, J.; Alonso, B. Seafloor Characterization and Backscatter Variability of the Almería Margin (Alboran Sea, SW Mediterranean) Based on High-Resolution Acoustic Data. *Mar. Geol.* **2008**, *250*, 1–18. [CrossRef]
65. D'Acremont, E.; Gorini, C.; Alonso, B.; Ammar, A.; El Abbassi, M.; de Batist, M.; Ceramicola, S.; Do Couto, D.; Ercilla, G.; Gutscher, M.; et al. Active sedimentation and tectonics in the South Alboran Sea: Preliminary results of the Marlboro and SARAS surveys. In Proceedings of the Exploring the Mediterranean: New Concepts in an Ancient Seaway, Barcelona, Spain, 8–11 April 2013.
66. Vázquez, J.-T.; Ercilla, G.; Catalán, M.; Do Couto, D.; Estrada, F.; Galindo-Zaldívar, J.; Juan, C.; Palomino, D.; Vegas, R.; Alonso, B.; et al. Ch.5, A Geological history for the Alboran Sea region. In *Alboran Sea and its Marine Resources*; Baéz, J.C., Vázquez, J.T., Caminas, J.A., Malouli, M., Eds.; Springer Nature: Cham, Switzerland, 2021; pp. 111–156. [CrossRef]
67. Parrilla, G.; Kinder, T.H.; Preller, R.H. Deep and Intermediate Mediterranean Water in the Western Alboran Sea. *Deep Sea Res. Part A. Oceanogr. Res. Pap.* **1986**, *33*, 55–88. [CrossRef]
68. Vargas-Yáñez, M.; García-Martínez, M.C.; Moya, F.; Balbín, R.; López-Jurado, J.L. Ch.4. The Oceanographic and Climatic Context. In *Alboran Sea and its Marine Resources*; Baéz, J.C., Vázquez, J.T., Caminas, J.A., Malouli, M., Eds.; Springer Nature: Cham, Switzerland, 2021; pp. 85–109. [CrossRef]
69. Millot, C. Circulation in the Western Mediterranean Sea. *J. Mar. Syst.* **1999**, *20*, 23–442. [CrossRef]
70. Sarhan, T.; Lafuente, J.; Vargas-Yáñez, M.; Vargas, J.; Plaza, F. UpwellingMechanisms in theNorthwesternAlboran Sea. *J. Mar. Syst.* **2000**, *23*, 317–331. [CrossRef]

71. Morán, X.A.G.; Taupier-Letage, I.; Vázquez-Domínguez, E.; Ruiz, S.; Arin, L.; Raimbault, P.; Estrada, M. Physical-Biological Coupling in the Algerian Basin (SW Mediterranean): Influence of Mesoscale Instabilities on the Biomass and Production of Phytoplankton and Bacterioplankton. *Deep Sea Res. Part I Oceanogr. Res. Pap.* **2001**, *48*, 405–437. [CrossRef]
72. Rueda, J.L.; Gofas, S.; Aguilar, R.; de la Torriente, A.; García Raso, J.E.; Lo Iacono, C.; Luque, Á.A.; Marina, P.; Mateo-Ramírez, Á.; Moya-Urbano, E.; et al. Chapter 10: Benthic fauna of littoral and deep-sea habitats of the Alboran Sea: A hotspot of biodiversity. In *Alboran Sea, Ecosystems and Marine Resources*; Báez, J.C., Vázquez, J.T., Camiñas, J.A., Malouli, M., Eds.; Springer Nature Series: Cham, Switzerland, 2021; pp. 285–358. [CrossRef]
73. Palomino, D.; Alonso, B.; Lo Iacono, C.; Casas, D.; D'Acremont, E.; Ercilla, G.; Gorini, C.; Vázquez, J.T. Seamounts and Seamount-like Structures of the Alborán Sea. In *Atlas of the Mediterranean Seamounts and Seamount Like Structures*; Würtz, M., Rovere, M., Eds.; IUCN: Gland, Switzerland; Málaga, Spain, 2015; pp. 21–58.
74. Vázquez, J.; Ercilla, G.; Alonso, B.; Juan, C.; Rueda, J.L.; Palomino, D.; Fernández-Salas, L.M.; Bárcenas, P.; Casas, D.G.; Díaz-del-Río-Español, V.; et al. Submarine Canyons and Related Features in the Alboran Sea: Continental Margins and Major Isolated Reliefs. Submarine Canyon Dynamics in the Mediterranean and Tributary Seas- An Integrated Geological, Oceanographic and Biological Perspective. In *Submarine Canyon Dynamics in the Mediterranean and Tributary Seas*; Briand, F., Ed.; CIESM Publisher: Villa Girasole, Monaco, 2015; Volume 47, pp. 183–196.
75. Wienberg, C. A deglacial cold-water coral boom in the Alboran Sea: From coral mounds and species dominance. In *Mediterranean Cold-Water Corals: Past, Present and Future, Coral Reefs of the World 9*; Orejas, C., Jiménez, C., Eds.; Springer: Cham, Switzerland, 2019; pp. 57–60.
76. Grosse, P.; van Wyk de Vries, B.; Petrinovic, I.A.; Euillades, P.A.; Alvarado, G. Morphometry and evolution of arc volcanoes. *Geology* **2009**, *37*, 651–654. [CrossRef]
77. Vázquez, J.T.; Estrada, F.; Vegas, R.; Ercilla, G.; d'Acremont, E.; Fernández-Salas, L.M.; Alonso, B.; Fernández-Puga, M.C.; Gomez-Ballesteros, M.; Gorini, C.; et al. Quaternary tectonics influence on the Adra continental slope morphology (Northern Alboran Sea). In *Una Aproximación Multidisciplinar al Estudio de las Fallas Activas, los Terremotos y el Riesgo Sísmico*; Álvarez-Gomez, J.A., Martín-González, F., Eds.; Segunda Reunión Ibérica Sobre Fallas Activas y Paleosismología: Murcia, Spain, 2014.
78. Thiem, Ø.; Ravagnan, E.; Fosså, J.H.; Berntsen, J. Food Supply Mechanisms for Cold-Water Corals along a Continental Shelf Edge. *J. Mar. Syst.* **2006**, *60*, 207–219. [CrossRef]
79. Addamo, A.M.; Vertino, A.; Stolarski, J.; García-Jiménez, R.; Taviani, M.; Machordom, A. Merging Scleractinian Genera: The Overwhelming Genetic Similarity between Solitary Desmophyllum and Colonial Lophelia. *BMC Evol. Biol.* **2016**, *16*, 108. [CrossRef]
80. Remia, A.; Taviani, M. Shallow-Buried Pleistocene Madrepora-Dominated Coral Mounds on a Muddy Continental Slope, Tuscan Archipelago, NE Tyrrhenian Sea. *Facies* **2005**, *50*, 419–425. [CrossRef]
81. Taviani, M.; Corselli, C.; Freiwald, A.; Malinverno, E.; Mastrototaro, F.; Remia, A.; Savini, A.; Tursi, A. CORAL Shipboard Staff. Rise, decline and ressurrection of deep-coral banks in the Mediterranean BassIn Results of 2002 Coral Mission in the Ionian Sea. In *Cold-Water Corals and Ecosystems*; Freiwald, A., Roberts, J.M., Eds.; Springer: Berlin/Heidelberg, Germany, 2005.
82. Savini, A.; Corselli, C. High-Resolution Bathymetry and Acoustic Geophysical Data from Santa Maria Di Leuca Cold Water Coral Province (Northern Ionian Sea—Apulian Continental Slope). *Deep Sea Res. Part II Top. Stud. Oceanogr.* **2010**, *57*, 326–344. [CrossRef]
83. Martorelli, E.; Petroni, G.; Chiocci, F.L. Party, and the P. S. Contourites Offshore Pantelleria Island (Sicily Channel, Mediterranean Sea): Depositional, Erosional and Biogenic Elements. *Geo-Mar. Lett.* **2011**, *31*, 481–493. [CrossRef]
84. Savini, A.; Vertino, A.; Marchese, F.; Beuck, L.; Freiwald, A. Mapping Cold-Water Coral Habitats at Different Scales within the Northern Ionian Sea (Central Mediterranean): An Assessment of Coral Coverage and Associated Vulnerability. *PLoS ONE* **2014**, *9*, e87108. [CrossRef] [PubMed]
85. Angeletti, L.; Castellan, G.; Montagna, P.; Remia, A.; Taviani, M. The "Corsica Channel Cold-Water Coral Province" (Mediterranean Sea). *Front. Mar. Sci.* **2020**, *7*, 661. [CrossRef]
86. Foubert, A.; Depreiter, D.; Beck, T.; Maignien, L.; Pannemans, B.; Frank, N.; Blamart, D.; Henriet, J.P. Carbonate mounds in a mud volcano province off northwest Morocco: Key to processes and controls. *Mar. Geol.* **2008**, *248*, 74–96. [CrossRef]
87. Wienberg, C.; Hebbeln, D.; Fink, H.G.; Mienis, F.; Dorschel, B.; Vertino, A.; López Correa, M.; Freiwald, A. Scleractinian Cold-Water Corals in the Gulf of Cádiz—First Clues about Their Spatial and Temporal Distribution. *Deep Sea Res. Part I Oceanogr. Res. Pap.* **2009**, *56*, 1873–1893. [CrossRef]
88. Palomino, D.; López-González, N.; Vázquez, J.T.; Fernández-Salas, L.M.; Rueda, J.L.; Sánchez-Leal, R.; Díaz-del-Río, V. Multidisciplinary Study of Mud Volcanoes and Diapirs and Their Relationship to Seepages and Bottom Currents in the Gulf of Cádiz Continental Slope (Northeastern Sector). *Mar. Geol.* **2016**, *378*, 196–212. [CrossRef]
89. Vandorpe, T.; Wienberg, C.; Hebbeln, D.; Van den Berghe, M.; Gaide, S.; Wintersteller, P.; Van Rooij, D. Multiple generations of buried cold-water coral mounds since the early-middle Pleistocene transition in the Atlantic Moroccan coral province, southern Gulf of Cadiz. *Palaeogeogr. Palaeoclimatol. Palaeoecol.* **2017**, *485*, 293–304. [CrossRef]
90. McCulloch, M.; Taviani, M.; Montagna, P.; López Correa, M.; Remia, A.; Mortimer, G. Proliferation and demise of deep-sea corals in the Mediterranean during the Younger Dryas. *Earth. Planet. Sci. Lett.* **2010**, *298*, 143–152. [CrossRef]

91. Juan, C. The Influence of Bottom Currents on the Sedimentary Evolution of the Alboran Sea during the Pliocene and Quaternary. Ph.D. Thesis, Departament d'Estratigrafia, Paleontologia I Geociències Marines, Universitat de Barcelona, Barcelona, Spain, 2016. Available online: http://hdl.handle.net/10803/400655 (accessed on 25 January 2022).
92. Chiocci, F.L.; Ercilla, G.; Torres, J. Stratal Architecture of Western Mediterranean Margins as the Result of the Stacking of Quaternary Lowstand Deposits below "Glacio-Eustatic Fluctuation Base-Level". *Sediment. Geol.* **1997**, *112*, 195–217. [CrossRef]
93. Lobo, F.J.; Ercilla, G.; Fernández Salas, L.; Gámez, D. Chapter 11 The Iberian Mediterranean Shelves. In *Geological Society*; Memoirs: London, UK, 2014; Volume 41, pp. 147–170. [CrossRef]
94. Braga, J.C.; Aguirre, J. *Calcareous algae of Cabo de Gata-Nijar Nature Park*; Instituto Geológico y Minero de España: Madrid, Spain, 2009; 208p, ISBN 978-84-613-2560-3.
95. Keegan, B. The macrofauna of maërl substrates of the West coast of Ireland. *Cah Biol. Mar.* **1974**, *15*, 513–530.
96. Hall-Spencer, J.M.; Atkinson, R.J.A. Upogebia Deltaura (Crustacea: Thalassinidea) in Clyde Sea Maerl Beds, Scotland. *J. Mar. Biol. Assoc. United Kingdom* **1999**, *79*, 871–880. [CrossRef]
97. Pereira-Filho, G.H.; Francini-Filho, R.B.; Pierozzi, I., Jr.; Pinheiro, H.T.; Bastos, A.C.; Moura, R.L.; Moraes, F.C.; Matheus, Z.; Bahia, R.G.; Amado-Filho, G.M. Sponges and fish facilitate succession from rhodolith beds to reefs. *Bull. Mar. Sci.* **2014**, *91*, 45–46. [CrossRef]
98. Amado-Filho, G.M.; Moura, R.L.; Bastos, A.C.; Francini-Filho, R.B.; Pereira-Filho, G.H.; Bahia, R.G.; Moraes, F.C.; Motta, F.S. Mesophotic cosystems of the unique South Atlantic atoll are composed by rhodolith beds and scattered consolidated reefs. *Mar. Biodiv.* **2016**, *46*, 407–420. [CrossRef]
99. Gofas, S.; Luque, A.A.; Salas, C.; Templado, J.; Pola, M.; Urra, J.; Brusa, V.S.; Verdes, A. Moluscos de Los Fondos de Cascajo Profundo de La Isla de Alborán (Proyecto LIFE+ INDEMARES Alborán), 2014. Available online: http://hdl.handle.net/10630/8321 (accessed on 25 January 2022).
100. De La Torriente, A.; Aguilar, R.; Serrano, A.; García, S.; Fernández Salas, L.; García Muñoz, M.; Punzón, A.; Arcos, J.; Sagarminaga, R. Sur de Almería Seco de Los Olivos. In *Proyecto LIFE+ INDEMARES*; del Ministerio de Agricultura, F.B., Medio Ambiente, A.y., Eds.; 2014; 102p, Available online: www.indemares.es (accessed on 25 January 2022).
101. Aguirre, J.; Braga, J.C.; Martín, J.M.; Puga-Bernabeu, A.; Pérez-Asensio, J.N.; Sánchez-Almazo, I.M.; Génio, L. An enigmatic kilometer-scale concentration of small mytilids (Late Miocene, Guadalquivir Basin, S Spain). *Palaeogeogr. Palaeoclimatol. Palaeoecol.* **2015**, *436*, 199–213. [CrossRef]
102. Taviani, M.; Bouchet, P.; Metivier, B.; Fontugne, M.; Delibrias, G. Intermediate steps of southwards faunal shifts testified by last glacial submerged thanatocoenoses in the Atlantic ocean. *Palaeogeogr. Palaeoclimatol. Palaeoecol.* **1991**, *86*, 331–338. [CrossRef]
103. Meadows, P.S.; Shand, P. Experimental Analysis of Byssus Thread Production by Mytilus Edulis and *Modiolus Modiolus* in Sediments. *Mar. Biol.* **1989**, *101*, 219–226. [CrossRef]
104. Seed, R.; Brown, R.A. Growth as a Strategy for Survival in Two Marine Bivalves, Cerastoderma Edule and *Modiolus Modiolus*. *J. Anim. Ecol.* **1978**, *47*, 283. [CrossRef]
105. Holt, T.J.; Rees, E.I.; Hawkins, S.J.; Seed, R. *Biogenic Reefs (Volume IX). An Overview of Dynamic and Sensitivity Characteristics for Conservation Management of Marine SACs*; Scottish Association for Marine Science: Oban, UK, 1998; 174p.
106. Rees, E.I.S.; Sanderson, W.G.; Mackie, A.S.Y.; Holt, R.H.F. Small-Scale Variation within a *Modiolus Modiolus* (Mollusca: Bivalvia) Reef in the Irish Sea. III. Crevice, Sediment Infauna and Epifauna from Targeted Cores. *J. Mar. Biol. Assoc. UK* **2008**, *88*, 151–156. [CrossRef]
107. Sanderson, W.G.; Holt, R.H.F.; Kay, L.; Ramsay, K.; Perrins, J.; Mcmath, A.J.; Rees, E.I.S. Small-Scale Variation within a *Modiolus Modiolus* (Mollusca: Bivalvia) Reef in the Irish Sea. II. Epifauna Recorded by Divers and Cameras. *J. Mar. Biol. Assoc. UK* **2008**, *88*, 143–149. [CrossRef]
108. Lindenbaum, C.; Bennell, J.D.; Rees, E.I.S.; Mcclean, D.; Cook, W.; Wheeler, A.J.; Sanderson, W.G. Small-Scale Variation within a *Modiolus Modiolus* (Mollusca: Bivalvia) Reef in the Irish Sea: I. Seabed Mapping and Reef Morphology. *J. Mar. Biol. Assoc. UK* **2008**, *88*, 133–141. [CrossRef]
109. Van Rooij, D.; De Mol, B.; Huvenne, V.; Ivanov, M.K.; Henriet, J.-P. Seismic evidence of current controlled sedimentation in the Belgica mound province, upper Porcupine slope, southwest of Ireland. *Mar. Geol.* **2003**, *195*, 31–53. [CrossRef]
110. Huvenne, V.A.I.; Bailey, W.R.; Shannon, P.M.; Naeth, J.; di Primio, R.; Henriet, J.-P.; Horsfield, B.; de Haas, H.; Wheeler, A.J.; Olu-Le Roy, K. The Magellan mound province in the Porcupine Basin. *Int. J. Earth Sci.* **2007**, *96*, 85–101. [CrossRef]
111. van Haren, H. Internal wave–zooplankton interactions in the Alboran Sea (W-Mediterranean). *J. Plankton Res.* **2014**, *36*, 1124–1134. [CrossRef]
112. O'Reilly, B.M.; Readman, P.W.; Shannon, P.M.; Jacob, A.W.B. A model for the development of a carbonate mound population in the Rockall Trough based on deep-towed sidescan sonar data. *Mar. Geol.* **2003**, *198*, 55–66. [CrossRef]
113. Huvenne, V.A.I.; De Mol, B.; Henriet, J.-P. A 3D seismic study of the morphology and spatial distribution of buried coral banks in the Porcupine Basin, SW of Ireland. *Mar. Geol.* **2003**, *198*, 5–25. [CrossRef]
114. De Haas, H.; Mienis, F.; Frank, N.; Richter, T.O.; Steinacher, R.; de Stigter, H.; van der Land, C.; van Weering, T.C.E. Morphology and Sedimentology of (Clustered) Cold-Water Coral Mounds at the South Rockall Trough Margins, NE Atlantic Ocean. *Facies* **2008**, *55*, 1–26. [CrossRef]
115. Hernández-Molina, F.J.; Serra, N.; Stow, D.A.V.; Llave, E.; Ercilla, G.; van Rooij, D. Along-Slope Oceanographic Processes and Sedimentary Products around the Iberian Margin. *Geo-Mar. Lett.* **2011**, *31*, 315–341. [CrossRef]

116. Ercilla, G.; Juan, C.; Periáñez, R.; Alonso, B.; Abril, J.M.; Estrada, F.; Casas, D.; Vázquez, J.T.; d'Acremont, E.; Gorini, C.; et al. Influence of Alongslope Processes on Modern Turbidite Systems and Canyons in the Alboran Sea (Southwestern Mediterranean). *DSRI* **2019**, *144*, 1–16. [CrossRef]
117. Glogowski, S.; Dullo, W.-C.; Feldens, P.; Liebetrau, V.; Reumont, J.; Hühnerbach, V.; Krastel, S.; Wynn, R.; Flögel, S. The Eugen Seibold Coral Mounds Offshore Western Morocco: Oceanographic and Bathymetric Boundary Conditions of a Newly Discovered Cold-Water Coral Province. *Geo-Mar. Lett.* **2015**, *35*, 1–13. [CrossRef]
118. Beyer, H.; Schenke, H.W.; Klenke, M.; Niederjasper, F. High resolution bathymetry of the eastern slope of the Porcupine Seabight. *Mar. Geol.* **2003**, *198*, 27–54. [CrossRef]
119. García, M.; Alonso, B.; Ercilla, G.; Gràcia, E. The tributary valley systems of the Almeria Canyon (Alboran Sea, SW Mediterranean): Sedimentary architecture. *Mar. Geol.* **2006**, *226*, 207–223. [CrossRef]
120. Huvenne, V.A.I.; Van Rooij, D.; De Mol, B.; Thierens, M.; O'Donnell, R.; Foubert, A. Sediment Dynamics and Palaeo-Environmental Context at Key Stages in the Challenger Cold-Water Coral Mound Formation: Clues from Sediment Deposits at the Mound Base. *Deep Sea Res. Part I Oceanogr. Res. Pap.* **2009**, *56*, 2263–2280. [CrossRef]